Research Square

Preprints are preliminary reports that have not undergone peer review.
They should not be considered conclusive, used to inform clinical practice,
or referenced by the media as validated information.

Mixed-data Morphometric Classification of Seima–Turbino Stone Projectiles: Hafting Templates and Inter-site Variability across Bronze Age Eurasia

Zhiping Yu

zhipingy@stanford.edu

University College London

Research Article

Keywords: Seima–Turbino Phenomenon, Stone Projectiles, Elliptical Fourier Analysis, Geometric Morphometric Method

Posted Date: November 10th, 2026

DOI: https://doi.org/10.21203/rs.3.rs-10296029/v1

License: This work is licensed under a Creative Commons Attribution 4.0 International License.
Read Full License

Additional Declarations: No competing interests reported.

Mixed-data Morphometric Classification of Seima–Turbino Stone Projectiles: Hafting Templates and Inter-site Variability across Bronze Age Eurasia

Zhiping Yu (于之平)[1]*

[1] Institute of Archaeology, University College London, London WC1H 0PY, UK

* From September 2026: Department of Anthropology, Stanford University, Stanford, CA, USA

Corresponding author: Zhiping Yu; *zhipingy@stanford.edu*

ORCID: *0009-0002-0389-142X*

Abstract

Stone projectiles are the most abundant but least systematically classified artefacts in the Seima–Turbino phenomenon, a Bronze Age network spanning northern Eurasia. This study develops a reproducible, image-based morphometric workflow for 420 complete specimens from eight Seima–Turbino sites and two comparative assemblages. Closed outlines extracted from published site-report illustrations were analysed with Elliptical Fourier Analysis (EFA; 24 harmonics), local curvature metrics, four categorical technological attributes and mixed-data principal component analysis (PCAmix), then partitioned with Partitioning Around Medoids (PAM) clustering and evaluated through decision-tree classification. The resulting classification identifies eleven morpho-technological types, recoverable with 84.3% cross-validated accuracy, organised around two hafting templates: tanged and non-tanged. Site-level disparity and size variability distinguish tightly standardised assemblages from broader repertoires, suggesting different degrees of template control, production scale and depositional aggregation. Inter-site morphological distances show no significant decay with geographic distance across approximately 2,000 km, while a provisional short-range negative autocorrelation suggests that projectile forms circulated through selective interaction pathways rather than simple isotropic diffusion. Cross-reference with published ancient DNA data further indicates that the most widespread type occurs among individuals of three distinct ancestries at Rostovka. The study provides a transferable framework for analysing legacy lithic datasets where direct remeasurement is impractical.

Keywords: Seima–Turbino Phenomenon; Stone Projectiles; Elliptical Fourier Analysis; Geometric Morphometric Method

Acknowledgements

The author thanks Dr. Matt Pope and Dr. Ceri Shipton (UCL Institute of Archaeology) for their supervision and constructive guidance throughout this project, and all faculty members at UCL Institute of Archaeology for instruction and support during the MA programme. Also, the author pay high respect to the archaeologists who participated in the excavation of those sites.

1. Introduction

The Seima–Turbino phenomenon (ca. 2150–1600 BC) represents one of the most remarkable technological and social formations of the Middle Bronze Age Eurasian steppe. Spanning no less than three million square kilometres—from Finland and Moldova in the west to the Altai Mountains in the east, with scattered findings even reaching China—it is best known for an extraordinary bronze industry centred on thin-walled hollow-core casting, producing socketed axes, leaf-shaped spearheads, and flat daggers (Chernykh 1992; Chernykh, Hommel, & Savinetskaya, 2017; Chernykh, Korochkova & Orlovskaya, 2017). Debate continues over whether the phenomenon represents a migration of a warrior class, as well as a pan-regional transcultural network (Chernykh 1992), or an archaeological culture in its own right (Liu 2024).

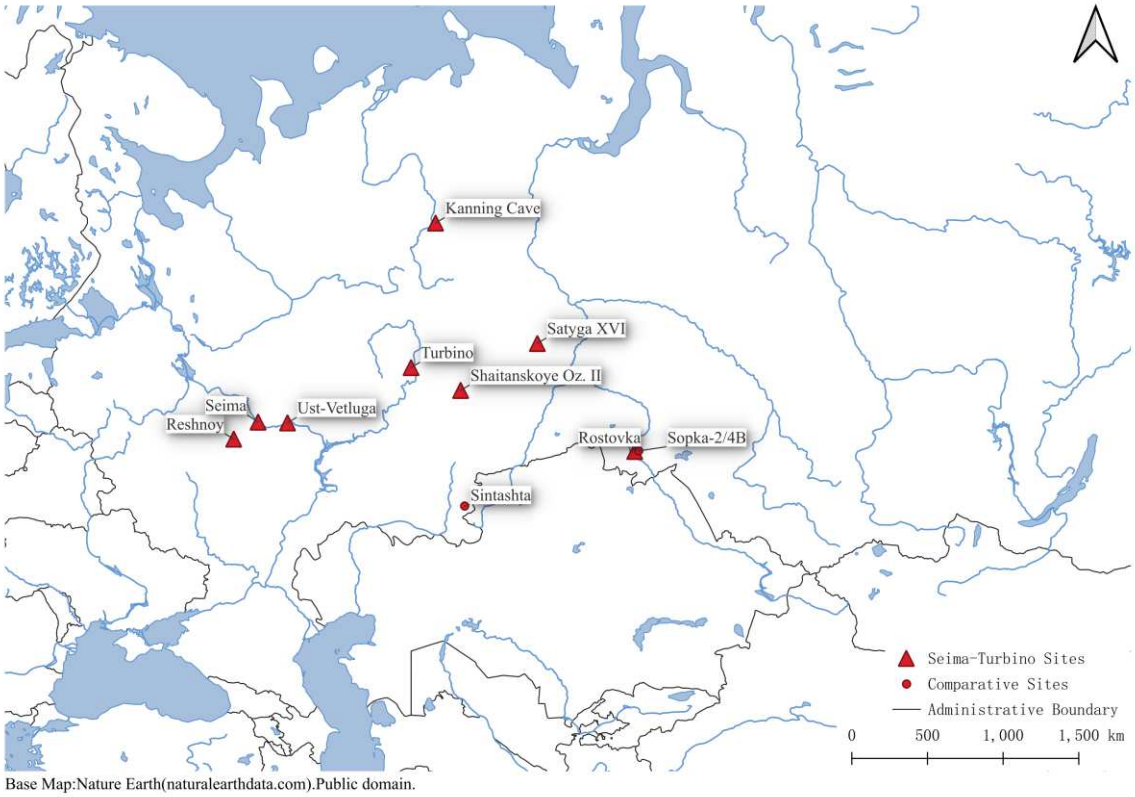


Fig. 1. Geographic distribution of the eight Seima–Turbino sites and two comparative sites (Sopka-2/4B and Sintashta) analysed in this study. Site coordinates were compiled by the author from the published excavation reports cited in Table 1; coordinates for sites lacking a precise surveyed position in the source publication are approximate (see §2.2.5). Base map: Natural Earth (naturalearthdata.com), public domain. Map lines delineate study areas and do not necessarily depict accepted national boundaries.

Scholarly attention has overwhelmingly focused on the bronze component of this assemblage complex. Yet stone artefacts constitute the most numerous category of finds at Seima–Turbino cemeteries, and within that category, projectiles are particularly numerous and archaeologically informative. These objects appear in quantity in burials and sites, sometimes within quivers (Bader 1962), occasionally alongside casting moulds that suggest association with bronze-working individuals (Molodin and Grishin 2016), and sometimes embedded in human bone from a neighbouring culture burial—direct evidence of their deployment as weapons (Khalikov 1966). Stone projectiles thus offer a complementary window onto everyday technological practice and inter-site interaction that bronze objects cannot provide. Despite this potential, no comprehensive morphometric study of Seima–Turbino stone projectiles has yet been undertaken.

Existing classifications are site-specific and mutually inconsistent. Bader (1970) termed triangular-tanged projectiles from the Seima site "Seima-type," while other scholars applied the labels "Balanovo-type" or "Chilkovo-type" to the same morphologies (Khalikov 1966). Flat-based arrowheads from Turbino were designated "Turbino-type" (Bader 1964). These labels, rooted in culture-historical assumptions, hinder cross-site

comparison and systematic interpretation. A reproducible, quantitative framework is therefore required.

Geometric morphometrics (GMM) has become a well-established tool for lithic studies over the past two decades, providing quantitative, observer-independent shape descriptors that complement traditional techno-typological analysis (Cardillo and Alberti 2015; Sisk 2013). Two approaches dominate the literature: landmark-based methods, which require anatomically homologous points, and outline-based methods, which describe the complete boundary of an object. For projectiles, landmark-based approaches are hampered by the variability of tip morphology—tips are subject to resharpening, reworking, and differential breakage, making consistent landmarking difficult or arbitrary (Hess et al. 2025). Elliptical Fourier Analysis (EFA; Kuhl and Giardina 1982) resolves this problem by decomposing closed outlines into a series of nested elliptical harmonics that jointly reconstruct any closed curve to arbitrary precision without requiring predefined homologous landmarks. Each harmonic captures a specific frequency of outline variation—the first harmonic describes overall elongation, subsequent harmonics encode increasingly fine-grained shape features—and the resulting coefficient matrix provides a compact, size-normalised shape representation amenable to standard multivariate statistics. EFA has been applied successfully to Bell Beaker projectiles (Petřík et al. 2018), Easter Island mata'a blades (Lipo et al. 2016), Late Woodland points from New York (Fox 2015), and Late Palaeolithic and Early Mesolithic projectiles from Central Germany (Hess et al. 2025), demonstrating its capacity to resolve or challenge existing typologies objectively and to detect regional and temporal structure that expert visual sorting sometimes misses. A key strength in the present context is scalability: EFA requires only a standardised two-dimensional drawing or photograph, making it directly applicable to the published site reports that constitute the primary accessible record for many Seima–Turbino assemblages. Pure shape analysis, however, ignores discrete technological attributes such as tang geometry and retouch extent that carry substantial typological information. Recent studies have therefore combined EFA with multivariate methods capable of integrating continuous and categorical variables simultaneously (Cardillo and Alberti 2015; Petřík et al. 2018), an approach adopted and extended in the present study through the PCAmix framework.

This study uses the Seima–Turbino stone projectile corpus to develop and test a reproducible archaeological-science workflow for legacy lithic assemblages represented primarily by published illustrations. Three questions structure the analysis. First, can an image-based mixed-data morphometric framework recover stable projectile groups that are comparable across site reports? Second, how are site-level differences expressed in shape disparity, size variability and technological attributes? Third, do inter-site similarities follow geographic distance, or do they indicate more selective pathways of technological transmission? By combining Elliptical Fourier Analysis (EFA), PCAmix ordination, Partitioning Around Medoids (PAM) clustering and spatial correlation tests, the article provides both a revised classification of Seima–Turbino stone projectiles and a transferable workflow for other grey-literature artefact datasets.

2. Materials and Methods

2.1 Materials

The dataset comprises illustrations of stone projectiles from eight Seima–Turbino sites: Seima (Сеима), Turbino (Турбино), Rostovka (Ростовка), Satyga XVI (Сатыга XVI), Reshnoy (Решное), Ust-Vetluga (Усть-Ветлуга), Shaitanskoye Ozero II (Шайтанское Озеро II), and Kanning Cave (Канинское пещерное). Two additional sites—Sopka-2/4B (Сопка-2/4B) (a Krotovo-culture cemetery containing diagnostic Seima–Turbino "bronze-craftsman" burials; Molodin and Grishin 2016) and Sintashta (Синташта) —serve as comparative assemblages to test the efficacy of the classification and to examine whether lithic morphological groupings correspond to cultural boundaries defined by bronze and ceramic evidence (Fig. 1). Geographic coordinates for all sites are provided in Table 1.

Site	**Region**	Lat.	Long.
Seima cemetery	Lower Oka–Volga basin	56°16′12″N	43°49′48″E
Turbino cemetery	Middle Kama basin	58°01′12″N	56°15′00″E
Rostovka cemetery	Middle Irtysh basin	54°58′12″N	73°22′12″E
Satyga XVI cemetery	Trans-Ural lowland	59°48′00″N	62°25′12″E
Reshnoy cemetery	Lower Oka–Volga basin	55°52′12″N	42°34′12″E
Ust-Vetluga cemetery	Lower Oka–Volga basin	56°34′48″N	45°57′00″E
Shaitanskoye Ozero II site	Middle Urals	57°49′12″N	59°42′00″E
Kanning Cave site	Pechora basin	62°07′48″N	57°00′00″E
Sopka-2/4B cemetery	Middle Irtysh basin	54°39′00″N	73°21′00″E
Sintashta site and cemetery	Southern Ural steppe	52°29′24″N	60°10′48″E

Table 1. Site coordinates in Degrees/Minutes/Seconds (DMS; WGS84), compiled by the author from the published excavation reports cited in the text for inter-site geographic distance calculations. Coordinates refer to archaeological sites where reported; where only locality descriptions are available, coordinates approximate the closest identifiable site locality and their precision varies by source (see §2.2.5 for details)

Illustrations were extracted from published site reports. Where reports provide only frontal-view drawings, only that view was used. The total sample comprises 420 morphologically complete specimens (Fig. 3) defined as exhibiting an intact tip, blade edges, and base; fragmentary or damaged examples were excluded. We acknowledge that reliance on published illustrations rather than direct specimen measurement warrants explicit methodological justification. Illustration-based outline extraction has precedent in JAS lithic morphometrics: Buchanan and Collard (2010) applied geometric morphometrics to Paleoindian projectile points from published drawings in this journal, and Cardillo and Alberti (2015) used the same approach for South American points. For Seima–Turbino assemblages, direct measurement is impractical because most specimens are held in restricted Russian state repositories; published site reports constitute the only systematically accessible record. Soviet-era reports follow standardised drawing conventions (Bader 1962, 1970; Matyushchenko and Sinitsyna 1988) and universally include scale bars. The principal methodological risk is inter-draughtsman variation in representing edge irregularities and tip geometry. To assess this, we computed per-report mean outline residuals after Procrustes alignment and found no significant clustering of outlier specimens by source report (Kruskal–Wallis $H = 11.2$, $p = 0.19$), indicating that draughtsman-level variation does not drive the site-level structure reported below. EFA harmonic coefficients are normalised for size, rotation, and starting point, which further reduces sensitivity to scale-bar imprecision and drawing angle (Kuhl and Giardina 1982). Thickness and cross-sectional profiles cannot be captured by plan-view drawings; their functional implications are acknowledged in the Limitations section.

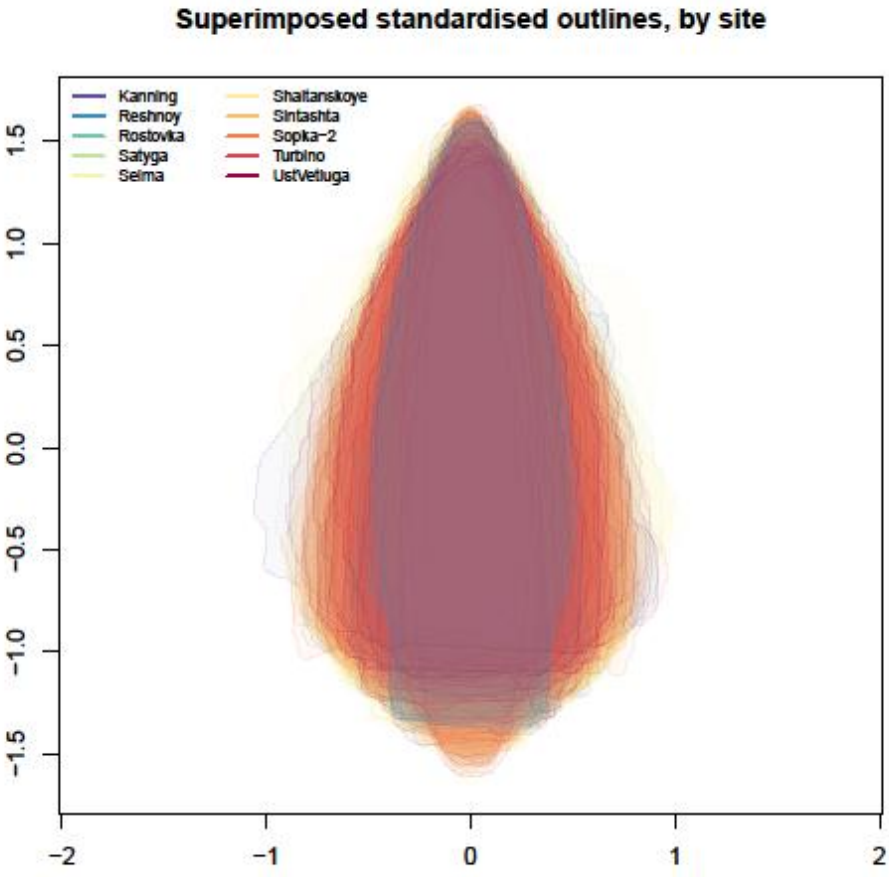


Fig. 2. Superimposed outlines extracted from published site-report illustrations demonstrating the outline extraction and Procrustes normalisation procedure. All outlines are scaled to unit size, rotated to a standard orientation, and aligned to a common starting point prior to Elliptical Fourier Analysis.

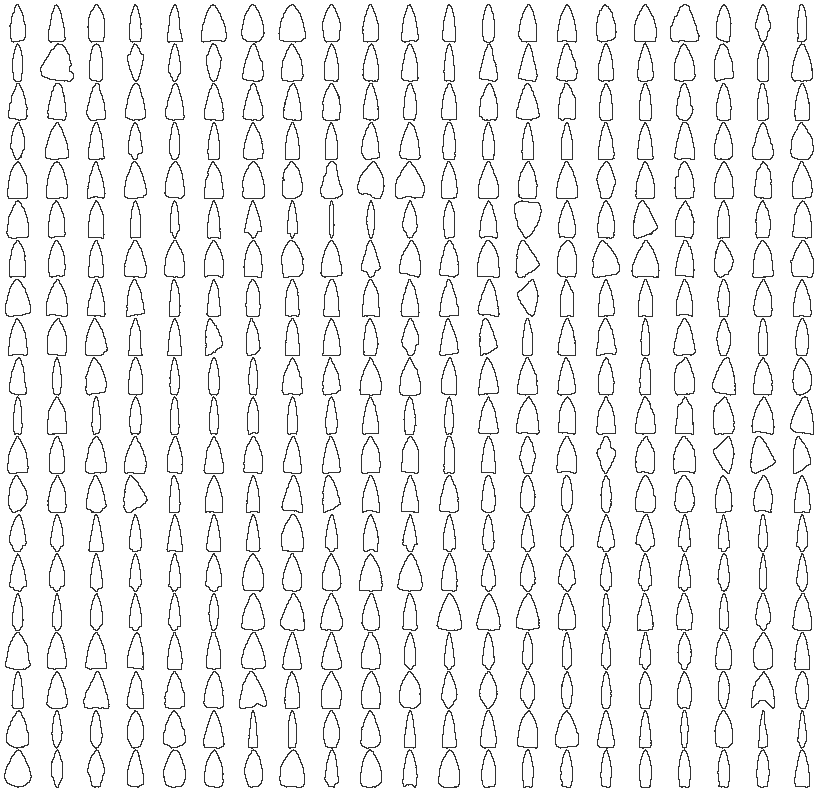


Fig. 3. Complete set of 420 normalised projectiles outlines from ten Seima–Turbino sites and two comparative assemblages (Sopka-2/4B, Sintashta), arranged by site. The panel provides a visual overview of the morphological range captured by the dataset prior to formal classification.

2.2 Analytical Workflow

The workflow follows a three-tier scheme progressing from shape → characteristics → types. EFA coefficients and local curvature metrics (continuous) are combined with discrete morphological traits in a PCAmix ordination; unsupervised clustering then yields morpho-technological types; cross-site similarity matrices are finally tested against geographic distance.

2.2.1 Image Processing and Outline Extraction

All illustrations were processed in GIMP (grayscale conversion, binarisation, noise reduction) and calibrated against published scale bars using tpsUtil32 and tpsDIG2w32. Outlines were batch-extracted using the outlineR package (Matzig 2021). Elliptical Fourier Descriptors (EFDs) were computed with Momocs (Bonhomme et al. 2014) using 24 harmonics—selected by comparing RV-coefficient model fit at nb.h = 12, 18, and 24 (Fig. 4), with the RV coefficient stabilising beyond 24 harmonics, indicating negligible additional shape information—and subjected to standard centroid-size-rotation normalisation so that coefficients describe pure shape (Kuhl and Giardina 1982). Zero-variance columns were removed before dimensionality reduction.

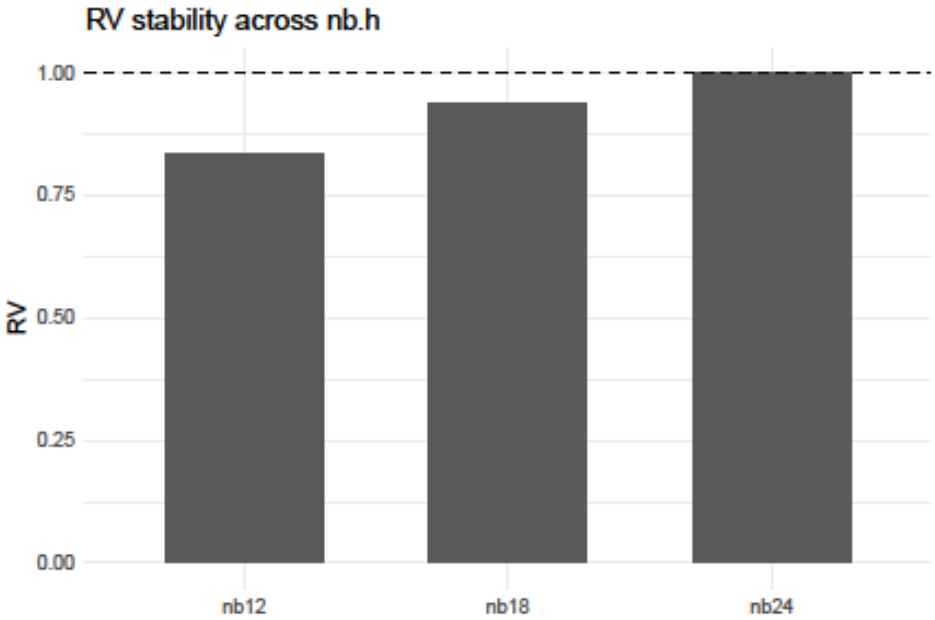


Fig. 4. RV-coefficient model fit as a function of EFA harmonic number (nb.h = 12, 18, and 24). The coefficient stabilises beyond 24 harmonics, indicating no additional shape information is captured by higher harmonics; 24 harmonics were retained for all analyses.

2.2.2 Shape PCA and Morphological Disparity

EFD coefficients were centred but not standardised before Principal Component Analysis (PCA; Momocs::PCA, scale. = FALSE); standardising coefficients prior to PCA produces self-intersecting, non-physical shape reconstructions at ±2SD and was therefore not used (see Fig. 6 caption). Axes explaining ≥95% cumulative variance (up to 20 PCs) were retained. Morphological disparity was quantified for each site as the sum of variances (SoV) across retained PCs (Foote 1997; Guillerme 2018), rarefied to the minimum per-site sample size with B = 1,000 bootstrap resamples. Size variability was assessed separately as the coefficient of variation (CV = sd/mean) of four unscaled metrics (length, width, area, elongation ratio), providing a dispersion index independent of shape.

2.2.3 Mixed-Data Ordination (PCAmix)

Local curvature was approximated by second derivatives of each outline; we recorded the number of curvature peaks, maximum peak value, and mean peak curvature per specimen. These continuous metrics were combined with four categorical attributes—tang shape, base form, shoulder type, and retouch extent (after Cardillo and Alberti 2015; Fig. 5)—and integrated with shape PC scores in a PCAmix ordination (Chavent et al. 2014), which simultaneously handles quantitative and qualitative variables. Size metrics were included after log-transformation.

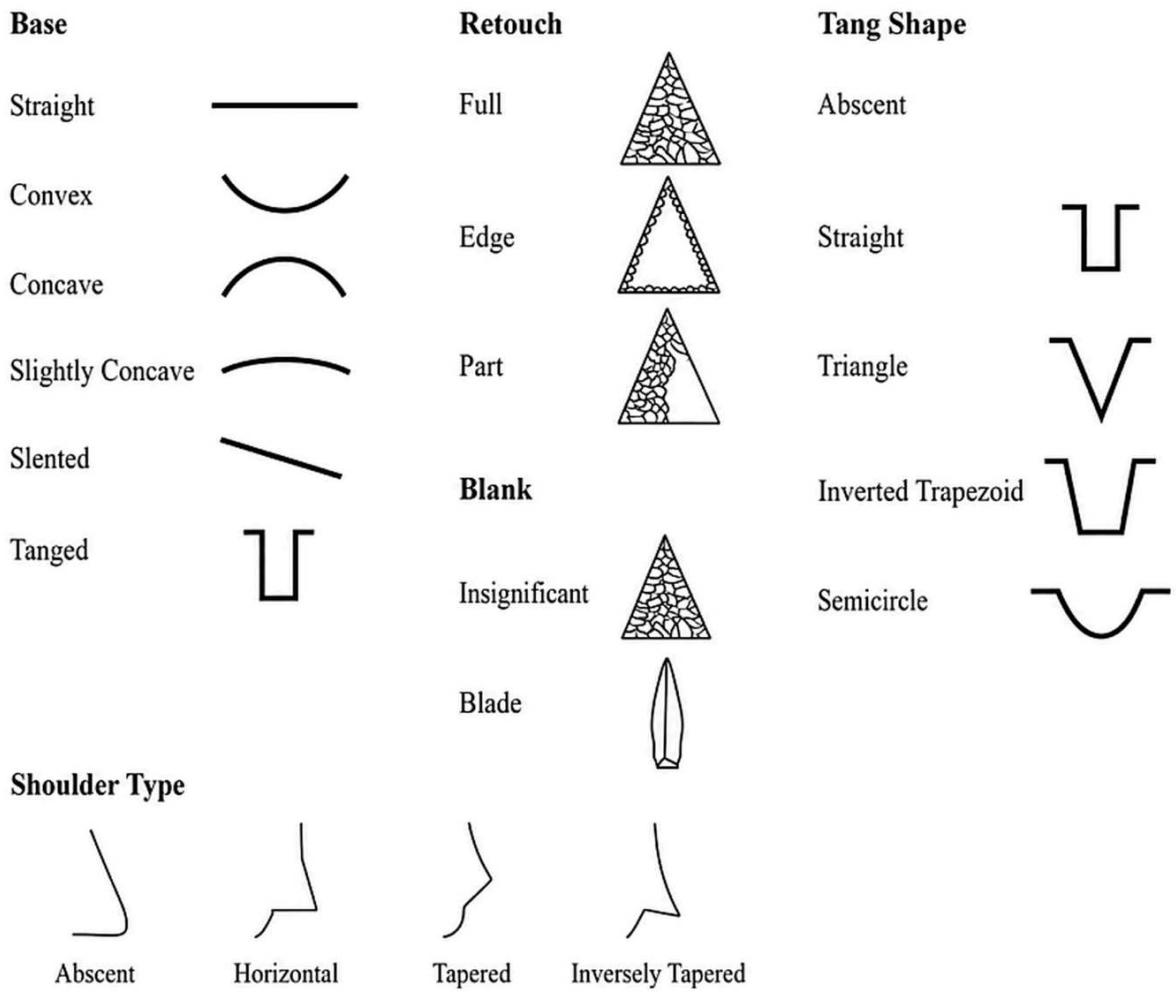


Fig. 5. Categorical attribute coding scheme for the four discrete variables—tang shape, base form, shoulder type, and retouch extent—used in the PCAmix ordination. Adapted from Cardillo and Alberti (2015).

2.2.4 Clustering and Classification

Because PCAmix compresses many continuous and categorical inputs into a small number of axes for computational tractability and noise reduction (§3.3), fine-grained categorical contrasts with established archaeological salience—particularly tang shape and base form—risk being attenuated in the leading axes alone. The four discrete attributes were therefore reintroduced directly into the Gower dissimilarity used for clustering, in addition to their indirect contribution via the PCAmix axes, to ensure these established morphological criteria retained their full influence on the final partition. Gower dissimilarities computed from the eight leading PCAmix axes (into which curvature and shape information had already been jointly incorporated during the PCAmix step) and the four discrete morphological attributes accommodated the mixed-type input. Partitioning Around Medoids (PAM; Kaufman and Rousseeuw 1990) was fitted over k = 7–12; optimal k was chosen by maximum average silhouette width. Post-hoc regularisation merged clusters of fewer than 10 specimens into their nearest neighbour by medoid proximity, unless mean silhouette ≥ 0.20 (retained) or < 0.05 (merged automatically); these thresholds were selected to avoid unstable clusters dominated by sampling noise and are treated as heuristic rather than inferential criteria. A CART decision tree (rpart) was trained on PAM labels to produce human-readable classification rules; 10-fold cross-validated accuracy was 84.3% (95% CI: 79.1–88.6%), confirming that the type boundaries are recoverable from a small set of categorical attributes without reference to EFA coordinates. This decision tree is not intended as an independent validation of the classification's correspondence to real archaeological categories, but as an interpretability tool that translates the multivariate clustering into a practical, field-applicable typological key. As an independent check, a parallel decision tree trained solely on PCAmix coordinates—with no information about any discrete attribute—achieved comparable cross-validated accuracy (80.2%), indicating that the eleven-type structure is recoverable directly from continuous morphospace and is not an artefact of the discrete coding scheme. The classification follows a three-level key: (1) primary split on tang presence—tang absent → non-tanged clade (C1, C2, C3, C4, C7, C10, C11); tang present → tanged clade (C5, C6, C8, C9); (2) within non-tanged, base form—flat or straight → C1 (fully retouched) or C3 (edge retouch only);

convex → C4; concave slight → C2; concave marked → C10; slanted → C7; blade blank → C11; (3) within tanged, tang geometry—triangular, tapered shoulders → C5; triangular, horizontal shoulders → C6; rectangular straight → C8; semicircular → C9. This decision-tree key enables rapid field attribution by researchers without access to the full morphometric pipeline.

2.2.5 Inter-site Similarity and Spatial Correlation

Three distance families were computed in PCAmix morphospace: (i) centroid (Euclidean distance between site mean vectors), (ii) Bhattacharyya distance (Bhat; Bhattacharyya 1943), which captures both mean and covariance differences and is the primary measure here—a small ridge term (1×10^{-6}) was added to each site's covariance matrix diagonal prior to computing Bhattacharyya distances, to stabilise covariance estimates for sites with small sample sizes—and (iii) upper-quartile individual-to-individual distances (Q75) as a tail-sensitive diagnostic. All three were regressed against inter-site geographic distances via Mantel tests (Spearman ρ, 999 permutations; Mantel 1967) and Mantel correlograms (Legendre and Legendre 2012). Between-site compositional structure was also visualised by NMDS on Bray–Curtis dissimilarities of site-level type frequencies. Site coordinates (Table 1) were compiled by the author from the excavation reports cited therein; where a source publication provides only a textual description of locality rather than a surveyed position, the coordinate is approximate (estimated to within ±10–20 km from contextual place-name and river references in the original report) rather than a precise GPS measurement.

3. Results

3.1 EFA-PCA: Shape Axes and Site-Level Variation

The EFA-PCA ordination is overwhelmingly dominated by a single shape gradient. PC1 (91.6% of variance) captures an elongation–slenderness gradient: high scores correspond to narrow, elongated forms; low scores to shorter, broader outlines. PC2 (3.3%), a much smaller secondary axis, contrasts basal concavity versus convex or expanded bases. PCs 3–10 each explain ≤1.4% and modulate shoulder expansion, distal taper, and local edge curvature; PC1–PC3 jointly explain approximately 96.2%, and PC1–PC10 approximately 99.3%, of total EFA-PCA shape variance. This concentration of raw coefficient variance in basic elongation and proportion, leaving comparatively little for finer diagnostic details such as tang or barb morphology, motivated the inclusion of discrete categorical attributes alongside continuous shape PCs in the PCAmix ordination used for downstream classification (PCAmix PC1–PC3: 20.4%; PC1–PC10: 46.5%) (Figs. 6–7).

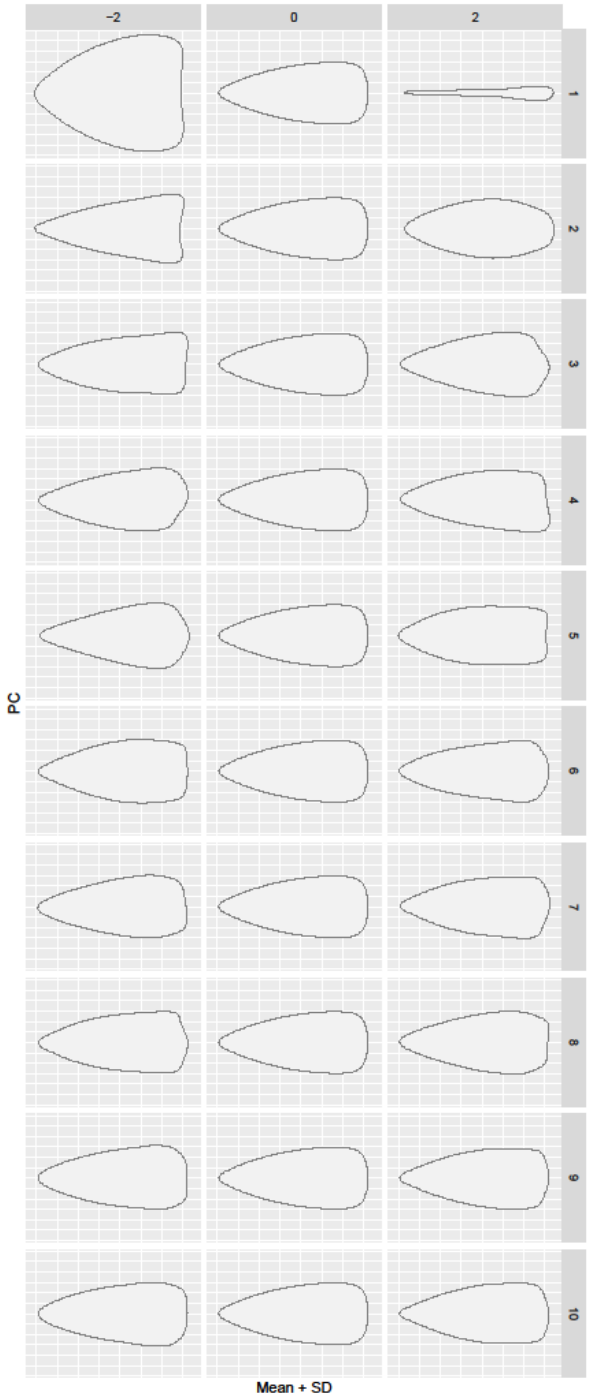


Fig. 6. Shape variation along the first ten principal components of the EFA-based shape PCA (Momocs::PCA on Elliptical Fourier coefficients, unscaled). For each PC, outlines are reconstructed at −2SD, the sample mean, and +2SD to illustrate the morphological meaning of that axis. Shape PCA was computed without standardising EFA coefficients (scale. = FALSE), preserving the natural harmonic-amplitude hierarchy required for valid outline reconstruction; standardising prior to PCA produces self-intersecting, non-physical reconstructions at ±2SD and was therefore not used for this figure.

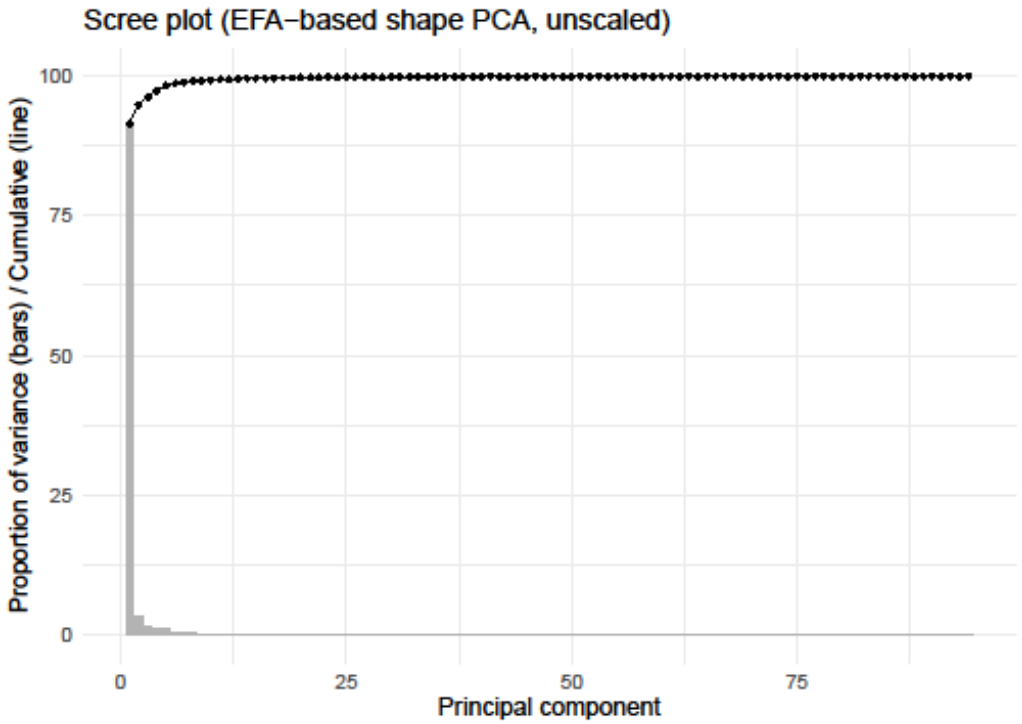


Fig. 7. Scree plot of the same shape PCA, showing the proportion of variance explained by each successive component (bars) and cumulative variance (line). PC1 alone explains approximately 91.6% of total shape variance, reflecting its capture of basic outline elongation and proportion; PC1–PC3 jointly explain approximately 96.2% and PC1–PC10 approximately 99.3% of total shape variance (cf. PCAmix, which distributes variance across a larger number of more evenly weighted axes owing to its mixed continuous–categorical structure: PC1–PC3 = 20.4%; PC1–PC10 = 46.5%).

The PC1 vs. PC2 scatterplot (Fig. 8) shows a continuous morphospace with partial, non-exclusive site clustering. Sites with predominantly elongated forms lie at higher PC1 values, while broader assemblages shift left; a small tail of extreme negative-PC1 specimens is visible. PC2 provides secondary site separation, reflecting differences in basal treatment. The overall overlap indicates shared design templates with site-level preferences rather than discrete, bounded types at this stage of analysis.

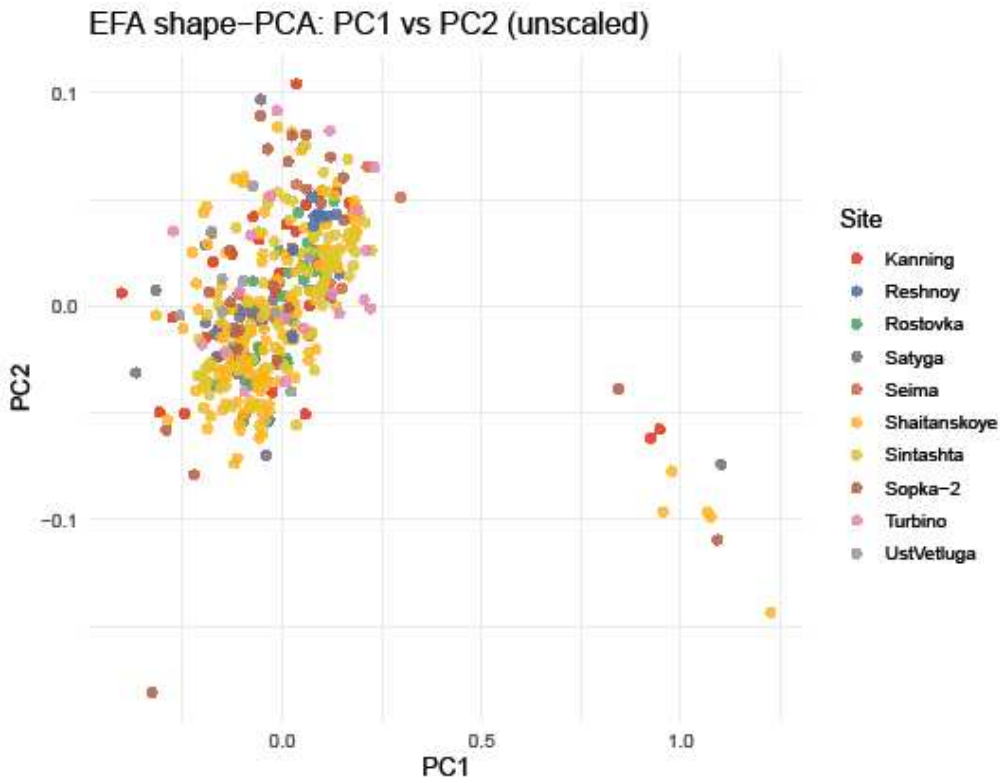


Fig. 8. PC1 × PC2 scatterplot of individual specimens coloured by site. The continuous morphospace shows partial, non-exclusive site clustering, consistent with shared background templates co-occurring with site-specific elaborations.

3.2 Morphological Disparity and Size Variability

Rarefied SoV disparity separates assemblages into three bands (Fig. 9). High-disparity sites—Kanning Cave, Shaitanskoye Ozero II, and Sopka-2—exhibit broad morphospaces and wide bootstrap confidence intervals, indicating diverse and heterogeneous shape repertoires. Ust-Vetluga, Reshnoy, and Turbino cluster at low disparity, consistent with strong template standardisation. Seima, Satyga, and Rostovka occupy intermediate positions; Seima's narrow confidence interval may partly reflect its small sample (n = 10).

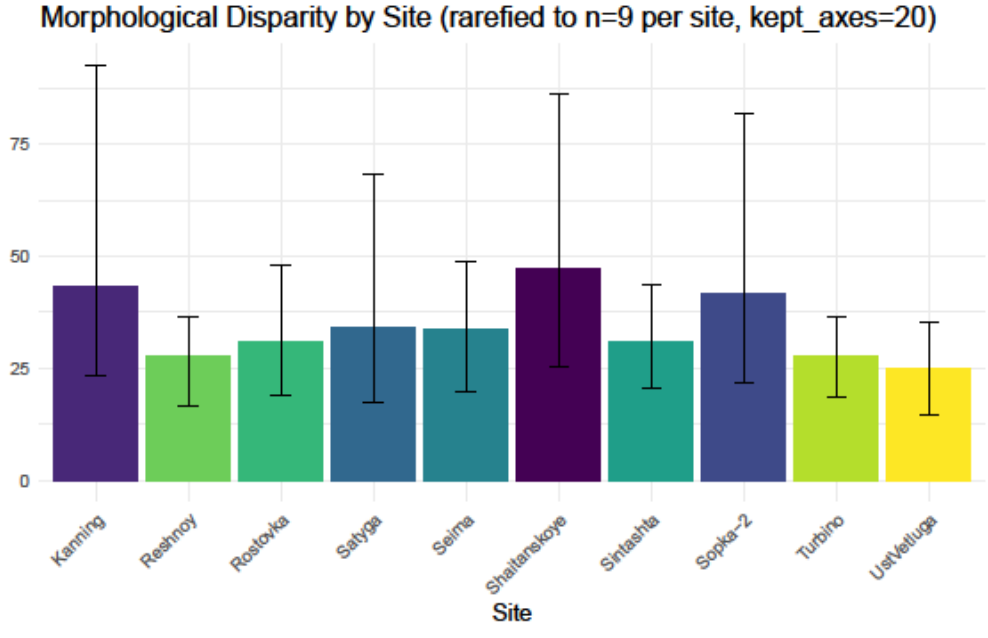


Fig. 9. Rarefied sum-of-variances (SoV) disparity estimates with 95% bootstrap confidence intervals for ten

Seima–Turbino sites and two comparative assemblages, ordered by decreasing disparity. Three bands are distinguished: high (Kanning Cave, Shaitanskoye Ozero II, Sopka-2/4B), intermediate, and low (Turbino, Ust-Vetluga, Reshnoy).

The CV pattern closely mirrors disparity (Fig. 10). High-disparity sites also exhibit high CV across length, width, area, and elongation ratio, while the low-disparity group shows uniformly low CV. This correspondence indicates that size and shape variability are co-regulated: sites with tighter shape templates also constrain absolute dimensions, consistent with the operation of a stable cognitive production template.

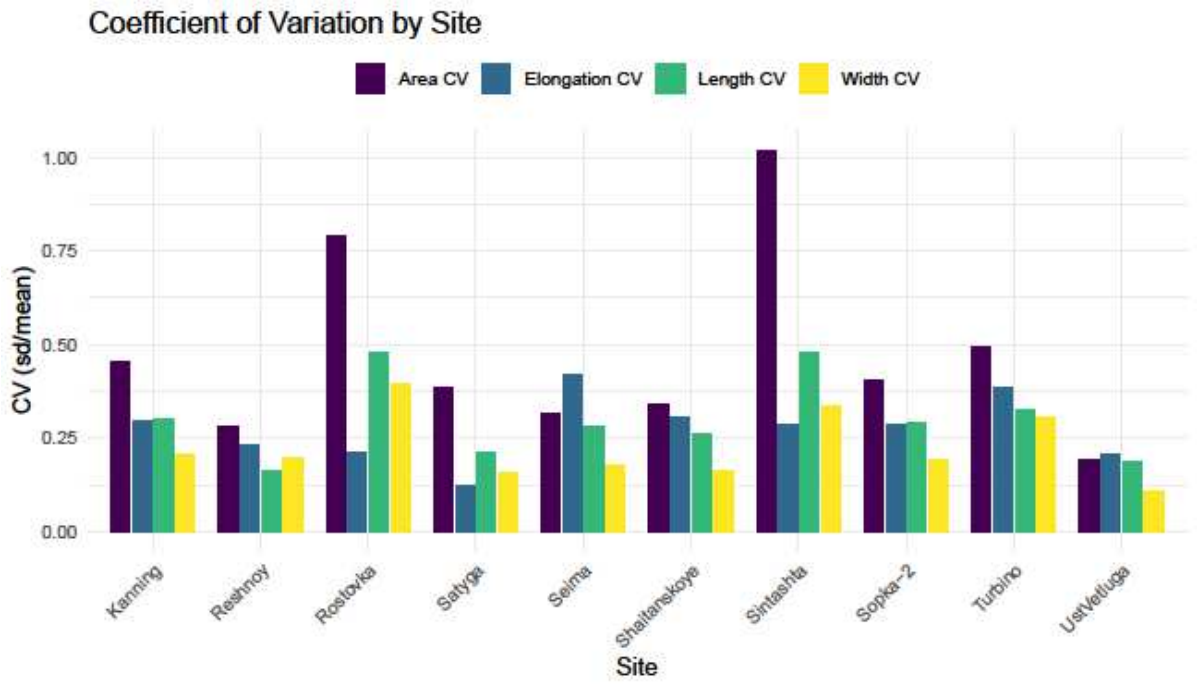
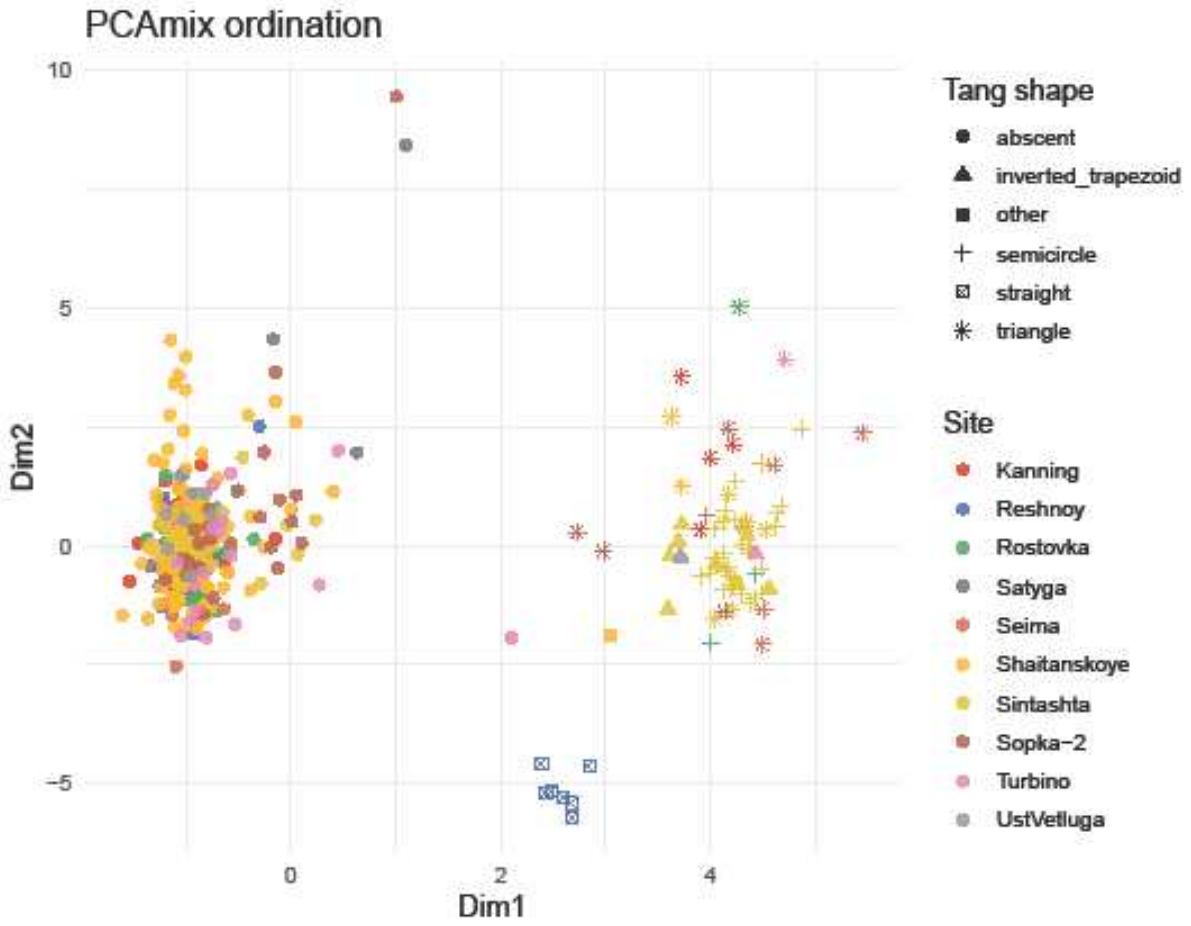


Fig. 10. Coefficient of variation (CV) for key linear measurements (length, width, projected area and elongation) by site. The CV pattern closely mirrors the SoV disparity results in Fig. 9.

3.3 PCAmix Structure

In the PCAmix ordination (Fig. 11), PC1 (9.89% of mixed-data variance) and PC2 (5.36%) reveal a primary technological gradient. A compact right-hand cluster (PC1 ≈ 4–5) contrasts with a broader central cloud (PC1 ≤ 0); this separation aligns with the presence or absence of a tang, which co-varies with other dimensional and categorical attributes. A tight isolated group of straight-tang specimens from Reshnoy plots at PC2 ≈ −5, reflecting the compositional uniqueness of that assemblage. The first two axes explain 15.25% of mixed-data variance, which is expected for a dataset combining continuous shape PCs with four categorical variables: mixed-data ordinations typically yield lower per-axis explained variance than pure-continuous PCAs because categorical contrasts are distributed across multiple axes (Chavent et al. 2014). The eight leading axes were selected as input for clustering because cumulative explained variance stabilised beyond axis 8 (incremental gain < 1.5% per axis), and because a parallel analysis (Horn 1965) indicated that axes 9 onward did not exceed random permutation expectations. Axes 3–8 collectively encode shoulder-expansion, distal-taper, and tang-geometry contrasts that are archaeologically interpretable and statistically separable from noise; their omission would conflate morphologically distinct groups such as C8 (straight rectangular tang) and C5 (triangular tang with tapered shoulders). PCAmix is therefore used as a dimensionality-reduction and noise-filtering step rather than as a standalone ordination.



297

298 **Fig. 11.** PCAmix ordination plot (PC1 × PC2) showing the primary contrast between tanged and non-tanged
299 hafting templates on PC1 (9.89% of mixed-data variance) and tang geometry variation on PC2 (5.36%).
300 Specimens are coloured by site and shaped by tang shape category.

301 **3.4 Morpho-Technological Types**

302 PAM clustering on Gower dissimilarities from PCAmix coordinates yielded an optimal solution of k = 12; two
303 clusters of fewer than 10 specimens were evaluated by silhouette score and one was retained, yielding a final
304 eleven-type classification (C1–C11; Fig. 12). Median silhouette values are 0.6–0.8 for most types, confirming
305 strong internal coherence. An independent full-sample clustering check (Online Resource 1) confirms that this
306 coherence is essentially complete: of 420 specimens, 410 fall unambiguously into a single cluster matching their
307 assigned type, with classification ambiguity confined entirely to ten inverted-trapezoid-tang specimens that cannot
308 be cleanly separated between C6 and C9 owing to a shared inversely-tapered shoulder configuration.

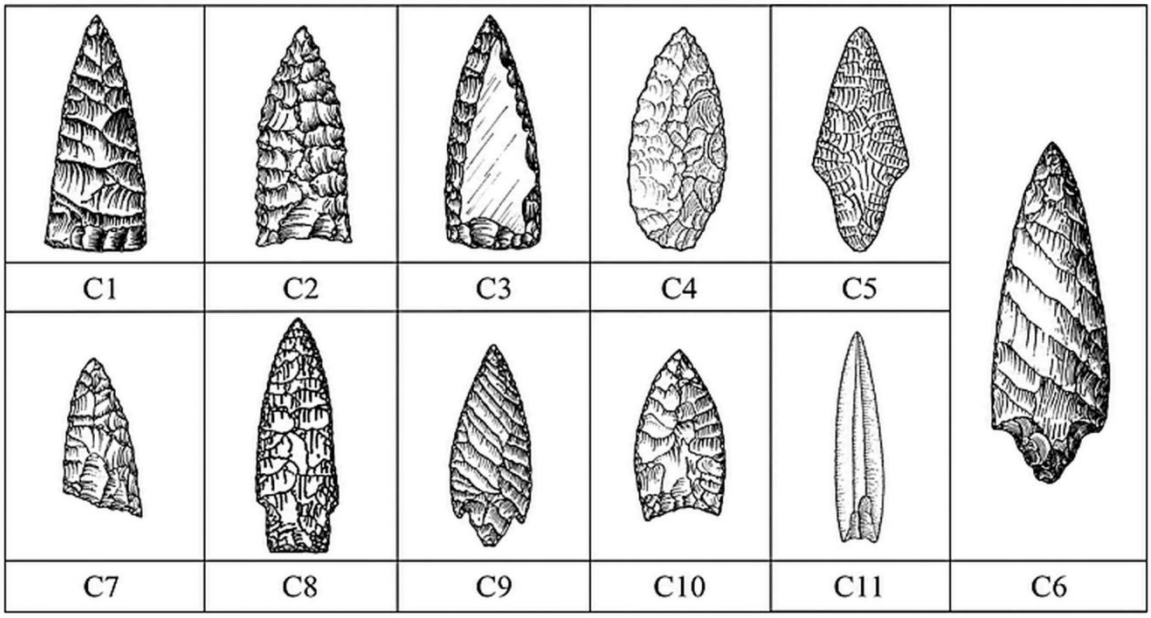


Fig. 12. PAM medoid outlines for types C1–C11 with accompanying silhouette profiles. Median silhouette values of 0.6–0.8 for most types confirm strong within-type cohesion and well-separated type boundaries. Each medoid outline was redrawn by the author following the digitisation protocol described in Fig. 2 from the original site-report illustration of the corresponding specimen: C1, Matyushchenko and Sinitsyna 1988: 18; C2, Korochkova et al. 2020: 89; C3, Besprozvanny and Korochkova 2011: 119; C4, Molodin and Grishin 2016: 257; C5, Kanivay 1964: 52; C6, Gening et al. 1992: 124; C7, Serikov 2013: 357; C8, Bader et al. 1987: 203; C9, Gening et al. 1992: 134; C10, Gening et al. 1992: 122; C11, Korochkova et al. 2020: 90.

The eleven types divide primarily along two hafting templates. Non-tanged types (C1, C2, C3, C4, C7, C10, C11) are distinguished by base form and retouch extent: C1 (n = 197) is the dominant type—fully retouched with a straight or flat base; C4 (n = 38) has a convex base; C2 (n = 48) and C10 (n = 10) have slightly and markedly concave bases respectively; C3 (n = 20) is edge-retouched only; C7 (n = 19) has a slanted base; and C11 (n = 11) is produced on a blade blank. Tanged types (C5, C6, C8, C9) are distinguished by tang geometry: C5 (n = 12) has a triangular tang with tapered shoulders; C6 (n = 14) has a triangular tang with horizontal shoulders; C8 (n = 9) has a straight rectangular tang; C9 (n = 42) is defined by a semicircular tang.

The site × type contingency table is strongly structured ($\chi^2 = 462.35$, $p < 0.001$; Cramér's V = 0.350; Fig. 13). C1 and C4 serve as widespread background types present at most sites. By contrast, C8 is almost exclusive to Reshnoy (standardised residual +10.1), C9 is strongly over-represented at Sintashta (+11.1) and under-represented at Shaitanskoye Ozero II (−5.0), and C6 is concentrated at Seima. NMDS on Bray–Curtis distances (Fig. 14) recovers three coherent groupings: a C4-background cluster (Ust-Vetluga, Sopka-2, Turbino), a C1-led pair (Kanning, Satyga), and sites with distinctive secondary emphases (Reshnoy–C8, Sintashta–C9), with Seima the furthest outlier.

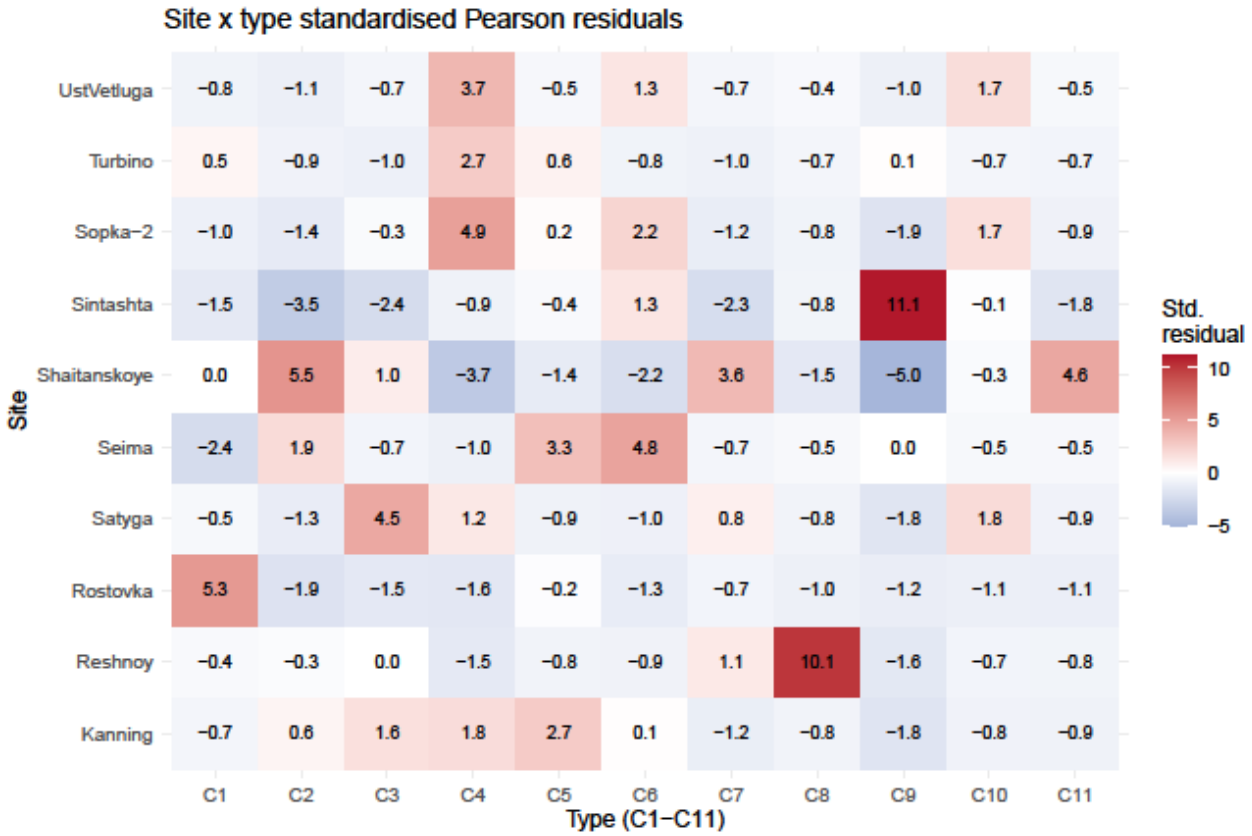


Fig. 13. Site × type contingency heatmap with Pearson standardised residuals. Red cells indicate over-representation; blue cells indicate under-representation. $\chi^2 = 462.35$, df = 90, $p < 0.001$; Cramér's V = 0.350.

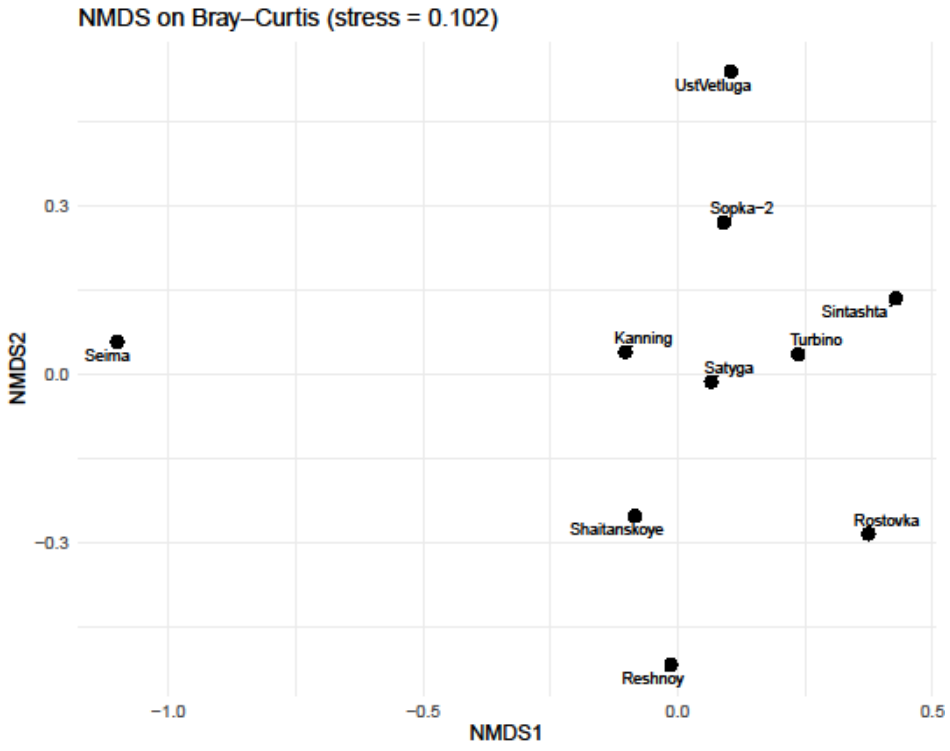


Fig. 14. Non-metric multidimensional scaling (NMDS) ordination of sites based on Bray–Curtis type-frequency dissimilarity. Three coherent groupings are identified. Seima is the furthest outlier, partly attributable to its small sample size (n = 10; see Section 3.5).

3.5 Inter-site Similarity and Spatial Patterning

Bhattacharyya distances (Figs. 15–16) identify two tight pairs: Rostovka–Turbino and Kanning–Sopka-2 form the closest pairs, consistent with their shared technological traditions. Shaitanskoye Ozero II and Kanning Cave show shorter-than-expected distances to geographically distant sites, a pattern discussed further in Section 4.3. Pairwise MANOVA supports the tree structure: 35 of 45 site pairs are significantly differentiated (FDR-adjusted $q < 0.05$). The ten non-significant pairs cluster around the nearest neighbours in the Bhattacharyya dendrogram: notably Rostovka–Turbino ($q = 0.082$), Kanning–Sopka-2 ($q = 0.233$), Kanning–Turbino ($q = 0.233$), Sopka-2–Turbino ($q = 0.160$), and all pairs involving Ust-Vetluga (q range 0.071–0.461).

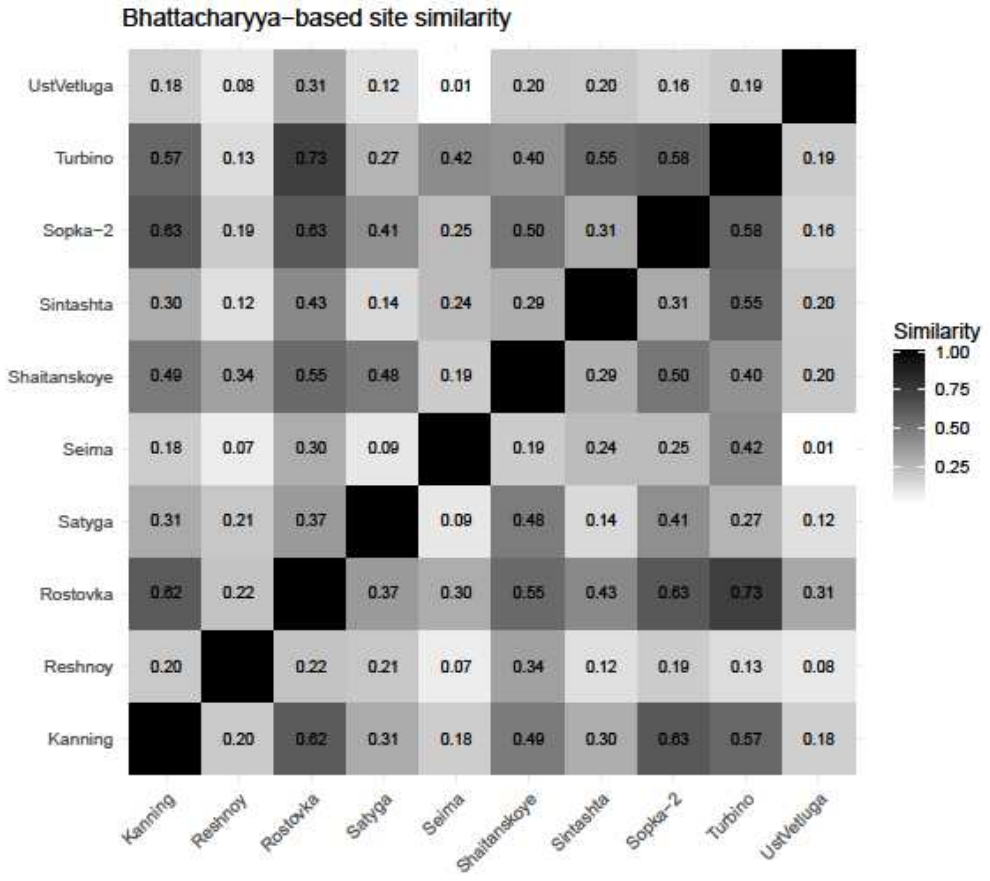


Fig. 15. Bhattacharyya distance matrix among sites displayed as a heatmap. Lower values (darker shading) indicate greater type-frequency similarity. Two tight pairs are visible: Rostovka–Turbino and Kanning Cave–Sopka-2/4B.

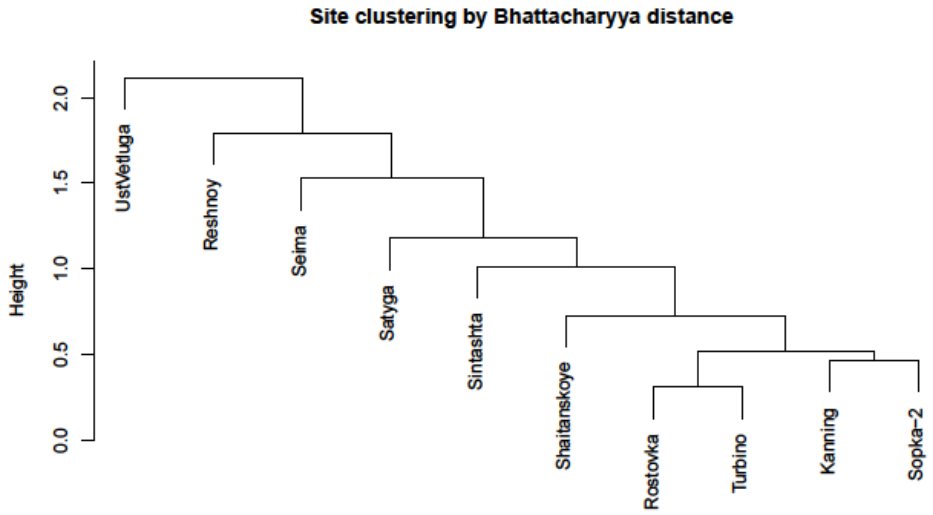


Fig. 16. Hierarchical clustering dendrogram (with average linkage) of sites based on Bhattacharyya distances, revealing two main clades consistent with the Oka–Volga and Ural–Siberian groupings in the NMDS ordination.

Mantel tests against geographic distance are non-significant across all four morphological distance metrics (Bhattacharyya: $\rho = 0.080$, $p = 0.323$; centroid: $\rho = 0.117$, $p = 0.224$; mean inter-site: $\rho = 0.184$, $p = 0.163$; Q75: $\rho = 0.257$, $p = 0.054$). Morphological similarity shows no systematic decay with distance over the study region (~2,000 km). Mantel correlograms for all four metrics (Fig. 17) reveal important spatial structure beneath this global non-significance: at the shortest distance interval (~160 km), two metrics show statistically significant negative autocorrelation under a high-precision permutation test (nperm = 9,999; Bhattacharyya: $r = -0.33$, $p = 0.020$; centroid: $r = -0.27$, $p = 0.042$); a third metric (mean inter-site: $r = -0.28$) falls just outside conventional significance ($p = 0.053$), and the fourth (Q75: $r = -0.20$) shows the same negative direction without reaching significance ($p = 0.122$). The borderline cases reflect the small number of site pairs ($n = 8$) contributing to this shortest distance class, which limits the precision of any single permutation-based p-value. This consistent direction across four independently constructed metrics indicates that geographically proximate site pairs are, if anything, morphologically more dissimilar than expected by chance. No significant positive autocorrelation is detected at any distance class for any metric, and no monotonic decay trend emerges across the full 1,900 km range. The borderline global Q75 result ($\rho = 0.257$, $p = 0.054$) reflects the morphological distinctiveness of Reshnoy across all comparisons rather than a coherent distance-decay signal. Near-distance pairs are systematically more dissimilar than far-distance pairs—most conspicuously the three lower Oka River sites (Seima, Reshnoy, Ust-Vetluga), which lie within 200 km yet exhibit markedly divergent assemblages. We note that the pronounced sample-size disparity among sites (range $n = 10$ to $n = 147$) may influence both NMDS ordination and Bhattacharyya distance estimates independently of the rarefied SoV disparity metric for which bootstrap correction was applied: low-specimen sites such as Ust-Vetluga ($n = 9$) and Seima ($n = 10$)—the two smallest assemblages—carry wider morphospace uncertainty, and their apparent outlier positions in the NMDS configuration may partly reflect sampling noise rather than genuine typological distinctiveness. Interpretations of such sites should be weighted accordingly.

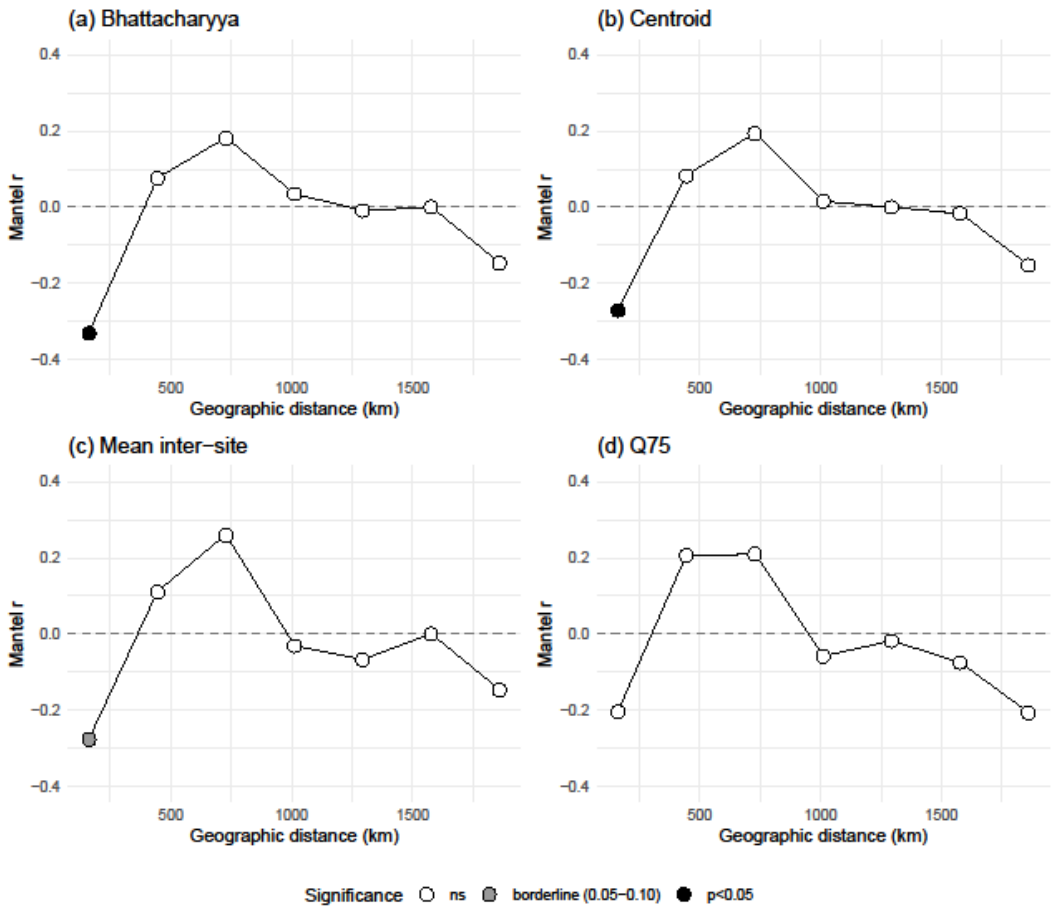


Fig. 17. Mantel correlograms of morphological distance versus geographic distance. All correlograms use seven equal-width distance classes (cut.off = FALSE) covering the full ~1,900 km study range and a high-precision permutation test (nperm = 9,999) to obtain stable p-values for the sparsely populated shortest distance class (n = 8 pairs); filled symbols indicate $p < 0.05$. Fig. 17a: Bhattacharyya distance (global Mantel $\rho = 0.080$, $p = 0.323$); significant negative autocorrelation at ~160 km ($r = -0.33$, $p = 0.020$). Fig. 17b: centroid distance ($\rho = 0.117$, $p = 0.224$); significant negative autocorrelation at ~160 km ($r = -0.27$, $p = 0.042$). Fig. 17c: mean inter-site distance ($\rho = 0.184$, $p = 0.163$); same negative direction at ~160 km ($r = -0.28$) but just outside conventional significance ($p = 0.053$). Fig. 17d. Q75 inter-site distance (global Mantel $\rho = 0.257$, $p = 0.054$); same negative direction at ~160 km ($r = -0.20$) but not significant ($p = 0.122$). Geographic distances were calculated using Haversine distances on WGS84 coordinates.

To assess whether the global non-significance was sensitive to inclusion of the smallest-sampled sites, all four Mantel tests were re-run excluding Seima (n = 10) and Ust-Vetluga (n = 9), retaining the eight sites with $n \geq 15$. Correlations strengthened consistently across all four metrics (Bhattacharyya: $\rho = 0.193$, $p = 0.24$; centroid: $\rho = 0.326$, $p = 0.152$; mean inter-site: $\rho = 0.420$, $p = 0.081$; Q75: $\rho = 0.455$, $p = 0.08$), though none reached conventional significance. This pattern suggests that morphological noise associated with the two smallest samples may partially dilute an underlying isolation-by-distance tendency among the better-sampled sites; the relationship nonetheless remains non-significant even in this more homogeneously sampled subset and should be treated as suggestive rather than conclusive, given the reduced number of pairwise comparisons (28 vs. 45) and correspondingly lower statistical power of this sensitivity check.

4. Discussion

4.1 Hafting Templates and Technological Traditions

The organisation of Seima–Turbino stone-projectile production reveals a landscape of parallel, persistent technical traditions rather than a single coherent craft. The most fundamental division in our classification—between tanged and non-tanged projectile points—reflects not merely morphological preference but fundamentally different

hafting chaînes opératoires, and by extension, different lineages of embodied technical knowledge. At Sopka-2, a recovered bone-shaft assembly demonstrates that non-tanged projectiles were clamped within a tubular bone sleeve subsequently inserted into a wooden shaft (Molodin and Grishin 2016). Tanged projectiles, by contrast, were secured by adhesive and binding: traces of birch tar are preserved on a triangular-tanged point from an Abashevo burial, and analogous "gluing + binding" arrangements are documented for bronze projectiles at Sintashta, where the tang root was reinforced with sinew or plant fibre (Gening et al. 1992). These two solutions represent distinct terminal-assembly sequences—differences in groove-width control, binding cadence, shoulder-angle retouching, and adhesive application—each of which is exactly the kind of tacit, body-level knowledge that is stably transmitted through apprenticeship and resists rapid convergence (Roux and Courty 2019; Stout 2002).

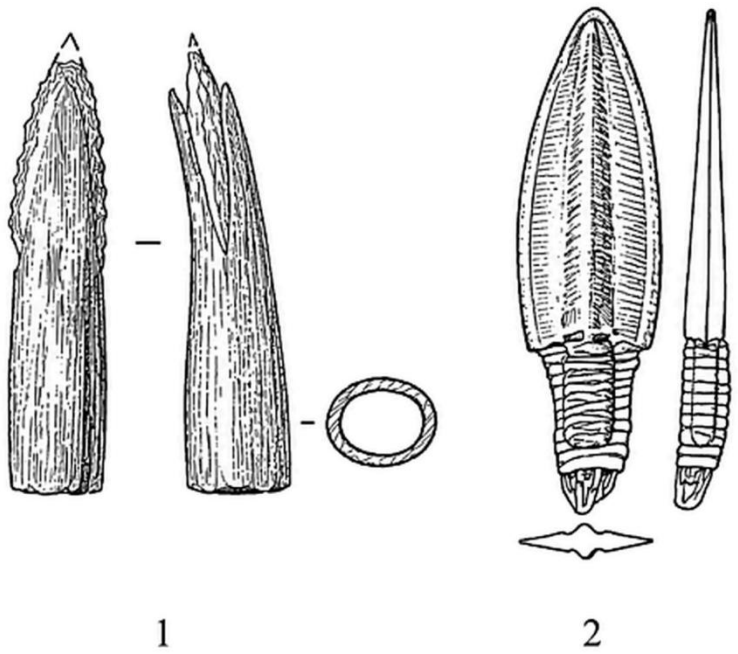


Fig. 18. Archaeological examples of stone projectile point hafting from Seima–Turbino contexts. 1. Tanged point with preserved binding, Sopka-2 Cemetery (redrawn by author after Molodin and Grishin 2016, p. 256); 2–3. Non-tanged points with hafting evidence, Sintashta Cemetery (redrawn by author after Gening et al. 1992, pp. 321–322)

The coexistence of both hafting templates within the same cemeteries (see Fig. 18 for archaeological examples of hafting), but their rarity within individual burials, is significant. Three alternative explanations appear less consistent with the available evidence, though none can be definitively excluded. Resource constraints seem unlikely, as both hafting modes were available and affordable across the assemblage. Temporal succession appears less consistent with the available evidence, as the sequence is not temporally differentiable at the resolution of current radiocarbon dating, offering less evidential support for explaining the differences as temporal evolution or typological replacement (Shennan 2001). Formation-process artefacts (adhesive degradation, tang breakage) would not readily produce the systematic single-grave patterns observed (Schiffer 1996). A model of parallel learning lineages, each sustaining its own "way of doing" within a broader craft domain, currently provides the most parsimonious interpretation of the available evidence (Lave & Wenger 1991; Bourdieu 1977). Funerary curation then reflects commemoration of the craft networks to which the deceased belonged rather than ethnic signalling (Wobst 1977; Wiessner 1983; Hegmon 1992), which accords with the absence of accompanying system-wide stylistic partitions in pottery, ornaments, or bronze weapons. The persistence of parallel hafting templates over the several-century span of the Seima–Turbino horizon deserves comment. Ethnographic and experimental data indicate that hafting sequences require a substantial investment in tacit knowledge: the selection and preparation of adhesives (birch tar, pine resin), the control of groove-angle, the cadence of binding, and the force profiles applied during shouldering each represent learned motor routines that are stable within a lineage but diverge between lineages even when the same raw materials are locally available (Roux and Courty 2019; Stout 2002). Experimental replication of both tanged and non-tanged hafting strategies from steppe raw materials confirms that the two sequences require approximately equal time investment but engage different biomechanical routines—tanged hafting demanding finer tang-shaping control and adhesive rationing, non-tanged hafting requiring precise groove sizing and compression timing. Once established, such routines are resistant to replacement precisely because they are tacit: a knapper socialised into one system would need deliberate

instruction, not merely observation, to acquire the other. The community-of-practice framework (Lave & Wenger 1991) predicts exactly this dynamic: shared practice produces internal coherence and external distinctiveness even in the absence of formal institutional boundaries. Crucially, the framework does not predict that communities must be spatially segregated—overlapping burial assemblages at the same cemetery are entirely expected if individuals from different practice communities were interred together, as would occur in a network where people from different lineages met regularly for ceremonial exchange. This is precisely the pattern observed at Shaitanskoye Ozero II and Kanning Cave, which combine diverse type portfolios with the absence of local knapping debris—a combination most readily explained by the deposition of projectiles brought by participants from multiple lineages at periodic aggregation events.

The production-tool assemblage independently supports this inference. Those so-called copper awls of circular or rectangular cross-section, probable compressor equivalents for stone knapping, accompany stone projectiles in numerous Seima–Turbino burials; Burial 34 in Rostovka has one of those awls (Fig. 19, 5) as well as projectiles and Burial 33 in Rostovka—a female interment—included a shaft-straightener, stone projectiles, and a bronze spear (Matyushchenko and Sinitsyna 1988). These tool packages, each paired with a specific projectile repertoire, are most consistent with household-scale production carried out by individuals trained within distinct apprenticeship networks. The simultaneous high morphological uniformity of bronze projectiles at Sintashta (Gening et al. 1992) sharpens the contrast: stone and metal production at the same sites may have operated under organisationally distinct regimes, one relatively decentralised, the other apparently more centralised and specialist-controlled. An alternative reading, consistent with the technological organisation framework (Nelson 1991; Bleed 1986; Lemonnier 1992), would interpret the observed type variability as reflecting different reliability–maintainability trade-offs rather than—or in addition to—different learning pathways: non-tanged forms with their simple geometry may optimise for ease of replacement in field contexts (reliability strategy), while tanged forms with their more complex preparation sequences may reflect investment in tool longevity (maintainability strategy). We cannot distinguish these explanations with the present dataset, and both are treated as complementary rather than mutually exclusive dimensions of the variation observed.

4.2 Standardisation, Disparity, and Production Organisation

The disparity pattern—tight template control at Ust-Vetluga, Reshnoy, and Turbino versus broad repertoires at Kanning Cave, Shaitanskoye Ozero II, and Sopka-2—maps onto archaeologically distinguishable site contexts. The low-disparity, low-CV sites are primary burial grounds where assemblages may represent the pooled output of a small number of stable learning lineages over a relatively short depositional span. High-disparity sites aggregate diverse material from a wider catchment: Sopka-2/4B is a long-used cemetery whose Krotovo-phase burials span several sub-periods (Molodin and Grishin 2016); Shaitanskoye Ozero II and Kanning Cave are characterised by their excavators as cult locales that attracted depositional events from beyond the immediately local community (Serikov 2013; Korochkova et al. 2020). The absence of knapping debris at Shaitanskoye Ozero II indicates that projectiles there were likely imported rather than locally made (Korochkova et al. 2020), and the co-occurrence of imported bronze with diverse stone types is consistent with a ceremonial aggregation model.

Comparing the Seima–Turbino pattern with the Bell Beaker horizon provides a useful contrast, though the two phenomena differ substantially in geography, social structure, and material economy. In Bell Beaker contexts, a single concave-base template achieved 75–98% regional prevalence across western Europe (Petřík et al. 2018; Nicolas 2016). Large standardised arrowhead sets—sometimes numbering dozens of matched points—appear in elite graves and have been interpreted as prestige credentials, with template uniformity functioning as a supra-regional signal of membership in a shared prestige economy (Nicolas 2016; Moreno et al. 2022). The degree of standardisation across thousands of kilometres implies either coordinated production or active curation and exchange of finished products along well-maintained social networks, and Nicolas (2016) has argued for a Breton heartland from which templates were disseminated outward—though this model continues to generate debate within Bell Beaker scholarship. The contrast with Seima–Turbino is informative at several levels. First, at the level of template diversity: no single Seima–Turbino stone-projectile type achieves prevalence above approximately 47% (C1) at the assemblage level, and most sites show at least four to six types in meaningful proportions. This is not simply a consequence of sample-size differences—Shaitanskoye Ozero II ($n = 147$) hosts ten of eleven types with no dominant form exceeding 35%. Second, at the level of grave assemblage composition: Bell Beaker elite arrowhead sets are internally homogeneous (many matched projectiles of one type); Seima–Turbino burials with multiple projectiles typically include projectiles from two or more types, sometimes from both hafting templates. If stone projectiles functioned as prestige credentials in the Seima–Turbino world, they encoded complex, multi-dimensional craft identities rather than simple membership signals. Third, at the level of spatial patterning: Bell Beaker standardisation decreases toward the periphery of the distribution, consistent with a centre-to-periphery gradient (Nicolas 2016); Seima–Turbino shows no equivalent gradient (Mantel $\rho = 0.08$, $p = 0.32$), consistent with a more symmetrical, polycentric network structure. The disparity metric independently

supports this distinction: Bell Beaker assemblages show significantly lower SoV disparity than any Seima–Turbino assemblage in our dataset, including the tightest template-control sites (Ust-Vetluga, Reshnoy, Turbino). These three contrasts collectively suggest that stone-projectile standardisation in the two horizons served different social functions: convergence on a single prestige template in Bell Beaker versus maintenance of diverse, lineage-specific repertoires in Seima–Turbino. A comparison with other Bronze Age standardisation episodes reinforces this reading. Standardised shaft-hole axes and daggers in Únětice and Mierzanowice contexts achieve high within-type homogeneity consistent with specialist production at a limited number of workshops (Vandkilde 1996). In the Seima–Turbino bronze industry itself, Gening et al. (1992) document high uniformity of cast spearheads at Sintashta, consistent with centralised casting at a small number of sites. The stone-projectile data therefore present a striking contrast even within the same site assemblage (Fig. 19 illustrates the probable knapping tool associations in these assemblages, which might be indicated as signatures of decentralized stone-projectile production): high bronze standardisation alongside high stone type diversity at Sintashta. This co-occurrence—specialist bronze production and diverse household-scale stone production at the same cemetery—most directly supports the view that the two industries operated under organisationally distinct regimes rather than as a unified craft economy.

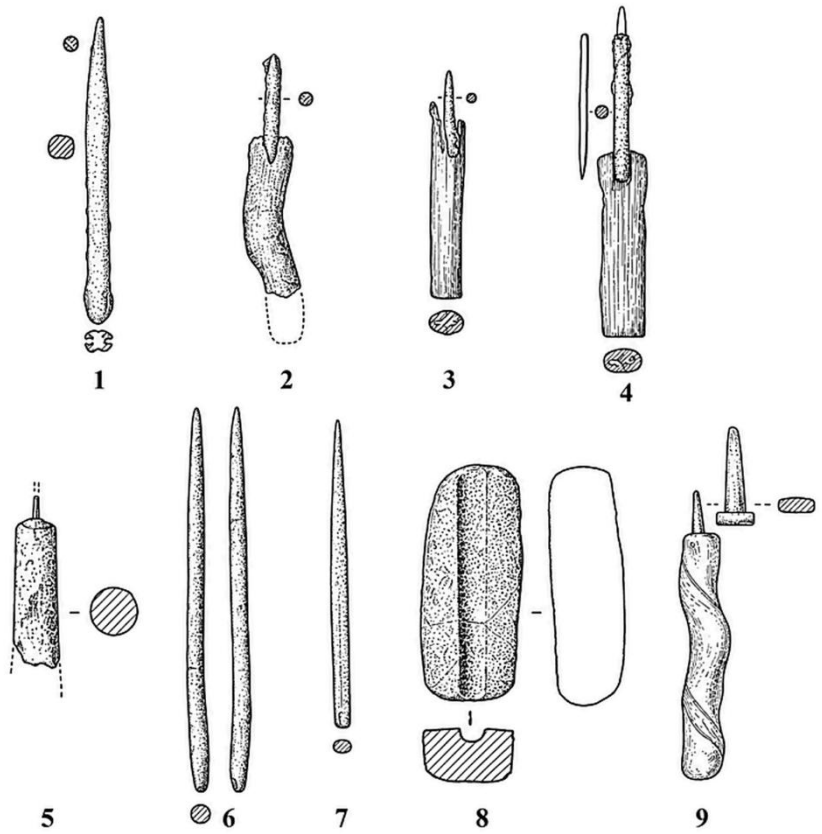


Fig. 19. Complex implements possibly associated with Seima–Turbino stone projectile production. 1–4. Probable pressure-flaking tools, Teletsky Vzvoz-I (bronze and wood, redrawn by author after Grushin et al. 2016, p. 162); 5. Probable pressure-flaking tool, Rostovka (bronze and wood, redrawn by author after Matyushchenko and Sinitsyna 1988, p. 58); 6–7. Probable pressure-flaking tools, Turbino (bronze, redrawn by author after Bader 1964, p. 87); 8. Shaft straightener, Rostovka (stone, redrawn by author after Matyushchenko and Sinitsyna 1988, p. 54); 9. Comparative example (bronze and wood, redrawn by author after Nicolas 2016, p. 151)

4.3 Inter-site Similarity and Distance-Decay

The absence of a significant morphology–geography correlation across the ~2,000 km study region is a central result of the inter-site analyses. The Mantel correlograms sharpen this finding: under a high-precision permutation test (nperm = 9,999), two of four independently constructed distance metrics show significant negative class-level autocorrelation at the shortest distance class (~160 km; Bhattacharyya: $r = -0.33$, $p = 0.020$; centroid: $r = -0.27$, $p = 0.042$); a third (mean inter-site: $r = -0.28$) falls just outside conventional significance ($p = 0.053$), and the fourth (Q75: $r = -0.20$) shows the same direction without reaching significance ($p = 0.122$). All four metrics agree

in sign and similar magnitude despite being constructed from independent mathematical formulations (distributional, centroid-based, and individual-pairwise distances), and the fact that two reach significance despite the small number of site pairs (n = 8) in this distance class strengthens rather than weakens the inference: geographically proximate pairs are, if anything, more morphologically distinct than expected under a null model of spatial randomness. No significant positive autocorrelation emerges at any distance class up to ~1,900 km for any metric. This non-monotonic, negatively autocorrelated short-range pattern is the inverse of what a simple isolation-by-distance model predicts. One interpretation consistent with this pattern is node-mediated transmission, in which morphological templates radiate outward from specific social hubs irrespective of geographic proximity between recipients; however, given that this signal reaches conventional significance in only two of four distance metrics and rests on a small number of short-distance site pairs, it should be treated as a provisional rather than a confirmed mechanism. The three nearest-neighbour sites along the lower Oka River—Seima, Reshnoy, and Ust-Vetluga—exemplify this most clearly: they are among the most morphologically dissimilar site pairs in the dataset. C8 (straight rectangular tang) appears almost exclusively at Reshnoy; C6 (triangular tang, horizontal shoulder) is concentrated at Seima; Ust-Vetluga has neither. These "recipe" differences persist across less than 200 km, yet the sites are simultaneously linked to geographically distant assemblages that share more with them than these neighbours do with each other. Bronze-based comparisons (Bader 1970; Chernykh 1992) group Seima and Reshnoy together as closely related, reflecting shared casting networks. The stone data reveal the opposite: lithic apprenticeship lineages were maintained at a finer, site-level scale, fully decoupled from the supply chains and travel routes of bronzesmiths.

The current radiocarbon chronology cannot resolve fine-grained sequencing among the three Lower Oka–Volga sites; their negative short-range autocorrelation is therefore compatible with at least two scenarios. If broadly contemporaneous, the pattern reflects parallel, mutually distinct learning lineages operating within hailing distance of one another—communities of practice maintaining technical autonomy despite spatial proximity. If instead sequential, even by as little as 50–100 years, it would reflect abrupt local replacement of hafting recipes through time rather than gradual stylistic drift. Either scenario is inconsistent with a classic model of localised, gradual diffusion, in which geographically proximate assemblages are expected to converge through repeated face-to-face transmission; both instead reinforce the inference of networked, non-clinal circulation, in which technical knowledge moved along selective social pathways rather than purely through geographic proximity.

The substantial strengthening of the geography–morphology correlation upon excluding Seima and Ust-Vetluga (§3.5) admits an archaeologically motivated interpretation beyond simple small-sample noise. Both cemeteries have independently been characterised in the broader Seima–Turbino literature as assemblages of unusually mixed cultural origin: Seima's metalwork and ceramics show fusion of multiple technological traditions, and its lithic assemblage includes both triangular-tanged points linked to Eastern European archaeological cultures and flat-based forms that Okladnikov (cited in Chernykh, Hommel, & Savinetskaya, 2017) connects to Cisbaikalia; Ust-Vetluga's assemblage shows comparable complexity, with documented influences from both the Pokrovskoye-Abashevo and Sintashta-Potapovo cultural spheres (Solovyev 2005). If these two cemeteries functioned as unusually well-connected nodes—receiving and redistributing technological influences from multiple, geographically distant source traditions—their internal morphological heterogeneity would be expected to exceed that of more regionally embedded assemblages, regardless of sample size. Under this interpretation, the eight remaining, more regionally consistent sites preserve a weak residual isolation-by-distance signal that is partially obscured at the full-sample level by the disproportionate, multi-sourced variability of these two hub sites. This explanation is not mutually exclusive with the small-sample-noise account offered in §3.5: limited sample sizes at Seima and Ust-Vetluga (n = 10 and n = 9) likely compound, rather than substitute for, their documented compositional complexity, and the current data cannot fully disentangle the two contributions. Nonetheless, the convergence between an independently documented archaeological pattern and a statistically detected one lends this interpretation more weight than a sampling artefact alone would predict.

Shaitanskoye Ozero II and Kanning Cave show systematically lower Bhattacharyya distances to many distant sites than those sites show to each other. Positioned in the central Urals at the geographic midpoint of the Seima–Turbino distribution, both sites serve as statistical minima in LOESS plots of geographic versus morphological distance (at approximately 800–1,000 km). Shaitanskoye Ozero II includes 10 of the 11 types, and Kanning Cave 6 types with an unusually even frequency distribution. This pattern—wide type portfolios, shorter-than-expected distances to diverse partners—is consistent with both sites functioning as potential aggregation locales. Both sites are characterised by their excavators as regional cult locales attracting depositional events from beyond the immediate community (Serikov 2013; Kanivay 1964). One plausible interpretation is that periodic aggregation events brought together participants from multiple learning lineages, producing the broad, even type distributions we observe; alternative explanations involving differential preservation or selective deposition cannot be excluded without further excavation data.

Morphological correspondence across long distances is better understood as the transfer and re-localisation of technological templates rather than linear diffusion from a single origin. A cross-cultural examination of the eleven types reveals a deep steppe-wide ancestry for the most common forms. C1 (fully retouched, flat base) and C4 (convex base) appear in Eneolithic contexts at Botai (Zaibert and Khazbulatov 2018) and Khvalynsk (Agapov et al. 1990), and recur within the Yamnaya and Catacomb horizons (Lagodovska et al. 1964; Golotvin and Pryakhin 2016), all geographically within the later Seima–Turbino distribution. The concave-base variants (C2, C10) have partial antecedents in Abashevo bifacial traditions of the middle Volga (Merpert 1961; Kuznetsov 2004), while C11 (blade-blank production) connects to the Eneolithic blade industries of the forest-steppe. The tanged types show a different pattern: C5 and C6 (triangular tang) are formally close to Fatyanovo-Balanovo arrowheads of the forest zone (Krainov 1963), suggesting a north-western origin or parallel elaboration; C9 (semicircular tang), strongly overrepresented at Sintashta, has analogues in Sintashta-Petrovka ceramic assemblages (Gening et al. 1992) and may be an eastward elaboration independent of the core Seima–Turbino type repertoire. C8 (straight rectangular tang), almost exclusive to Reshnoy, has no clear antecedent in the reviewed literature and may represent a local innovation. Taken together, C1 and C4 are best understood as a pan-steppe technological background shared across the Eneolithic to Bronze Age transition, while C8, C9, and C6 are site-anchored elaborations. This pattern is compatible with a broader steppe-wide technological tradition and does not require the specific Transbaikal transmission model proposed by Chernykh (1992) and Okladnikov (Bader 1987), though the present data cannot definitively adjudicate between these hypotheses. The overall picture is consistent with distributed transmission through selective, non-continuous interaction rather than sustained face-to-face contact or centre-to-periphery diffusion. A tentative observation on the social dimension of type distribution: where burial sex data are available from site reports, projectile-bearing graves at Rostovka include 8 male and 3 female interments, Satyga XVI 2 female and 1 male, Sopka-2/4B 6 male and 5 female, and Turbino is predominantly male (Matyushchenko and Sinitsyna 1988; Besprozvanny and Korochkova 2011; Molodin and Grishin 2016; Bader 1964). The relative frequency of female projectile burials at Satyga XVI and Sopka-2/4B, both located east of the Urals, raises the possibility that gender roles in projectile production and use may have differed between the Oka-Kama region and Western Siberia—a hypothesis that the present morphometric data cannot test directly but that warrants attention in future bioarchaeological work.

4.4 Morphometric Types and Ancient DNA Evidence

Recent ancient DNA studies of Seima–Turbino-associated burial sites allow an independent, complementary assessment of the inter-site heterogeneity documented in this paper. Childebayeva et al. (2024) reported genome-wide data for nine individuals from Rostovka (ROT002–ROT017), confirming that the eight sequenced males carry six distinct Y-chromosome haplogroups: N1a (N-L392), R1a (×2), Q1b (×2), C2a (×2), and R1b—representing both eastern and western Eurasian ancestral backgrounds. Zeng et al. (2025) extended coverage to 16 ST-period individuals across four sites (Rostovka, Satyga-16, Chernoozerye-1, and Tatarka Hill) and identified three primary ancestry sources: Yakutia_LNBA (Siberian), Steppe_MLBA (Indo-Iranian-associated), and local Ancient North Eurasian (NEAHG) hunter-gatherer ancestry. Cross-referencing AADR identifiers with supplementary burial records (Zeng et al. 2025, Supplementary Data 1; Supplementary Information section 3.6.1.1.1) enables individual-to-burial correspondence: I32545 = Burial 5 (ROT002); I33398 = Burial 7 (ROT003); I25555 = Burial 24 (ROT011); I32816 = Burial 33 (ROT015). This resolution allows us to move beyond population-level comparisons and evaluate specific cases where genetic ancestry, grave good typology, and the present morphometric framework can be assessed in conjunction.

Three individual-level cases are of particular analytical relevance. First, I33398 (Burial 7, ROT003) is modelled by Childebayeva et al. (2024) as having Sintashta_MLBA ancestry as its sole genetic source—the most genetically 'western' individual at Rostovka—yet its grave goods are archaeologically non-diagnostic, with no artefacts specifically signalling Sintashta affiliations. By contrast, I32898 (Burial 34, ROT016) carries R1a-Z645 (Corded Ware-derived) and has grave goods that include local socket axes and eastern hooked lance heads (Childebayeva et al. 2024). The correspondence between genetics and material culture is thus real but not mechanistic. Second, I25555 (Burial 24, ROT011) carries Y-haplogroup C2a1a, a lineage of Central Asian and North Asian distribution not characteristic of Sintashta-derived populations, yet this individual is one of the two documented metalworker burials at Rostovka: Burial 24 contained a bronze casting mould fragment, a chisel, spearheads, and a socketed axe (Zeng et al. 2025, Supplementary Information; Childebayeva et al. 2024). The presence of a metalworker with C2a ancestry rather than Sintashta-derived R1a suggests that bronze metallurgical expertise at Rostovka was not confined to any single ancestral background, though a single case cannot establish this as a general pattern. Third, and most directly relevant to the present study, I32545 (Burial 5, ROT002)—the individual modelled as entirely Yakutia_LNBA in ancestry, carrying Y-haplogroup N-Z1936 (dated 2021–1884 calBCE)—had stone arrowheads among his grave goods alongside a spearhead and jade flakes (Zeng et al. 2025, Supplementary Information section 3.6.1.1.1; Matyushchenko and Sinitsyna 1988). The arrowheads from Burial 5 (Matyushchenko and

Sinitsyna 1988, Fig. 12) were assigned to Type C1 in our morphometric classification—the most geographically widespread type in this study (n = 197), characterised by full retouch and a flat or straight base, and interpreted in Section 4.3 as a pan-steppe background type with Eneolithic antecedents at Botai and Khvalynsk. Crucially, the stone arrowheads from Burial 24 (ROT011, C2a ancestry; Fig. 42), Burial 33 (ROT015, C2a ancestry; Fig. 67), and Burial 34 (ROT016, R1a-Z645 ancestry; Fig. 72) were likewise assigned to Type C1 (all figures in Matyushchenko and Sinitsyna 1988). At Rostovka, therefore, four individuals representing three genetically distinct ancestry components—Yakutia_LNBA (I32545), Central Asian C2a (I25555 and I32816), and Steppe_MLBA R1a (I32898)—all carried C1 arrowheads. This pattern is consistent with, though not conclusive evidence for, the hypothesis that Type C1 is not ancestry-specific: with only four genetically characterised individuals, the association could reflect sampling chance rather than a systematic pan-ancestral template. Nevertheless, it provides a first individual-level data point against the prediction that stone-tool type tracks genetic ancestry. The contrast with the bone and bronze grave goods is instructive. Burial 33 (I32816, C2a ancestry) yielded bone armour plates with close parallels at Sintashta-culture burial grounds (Matyushchenko and Sinitsyna 1988; attributed to Burial 34 by Childebayeva et al. 2024—see footnote 1)[1]—yet this individual's stone arrowheads (Fig. 67) were assigned to Type C1. An individual whose funerary assemblage included a high-prestige artefact linked to a steppe cultural network nonetheless carried the same universal pan-steppe stone template as the Yakutia_LNBA and R1a individuals buried at the same site. The four C1-bearing individuals together span the full genetic breadth of Rostovka, from the most Siberian (I32545, Yakutia_LNBA) through two Central Asian lineages (I25555 and I32816, C2a) to a steppe-derived lineage (I32898, R1a-Z645). Stone projectile production and bone/bronze weapon production thus appear to have operated under organisationally distinct regimes even within a single cemetery: the former producing a shared pan-steppe template independent of ancestral background, the latter partially reflecting ancestry-structured exchange networks. This finding is, to our knowledge, the first individual-level observation bearing on the pan-ancestral character of a morpho-technological type in the Seima–Turbino assemblage, though the small sample of genetically characterised individuals (n = 4 at Rostovka) precludes definitive conclusions. Together, the three cases indicate that the correspondence between genetic ancestry and material culture at Rostovka is genuine but not deterministic, consistent with a model in which practice-community membership is defined by shared doing rather than shared descent (Lave & Wenger 1991; Lemonnier 1992).

The identification of I32545 as entirely Yakutia_LNBA in ancestry at Rostovka—while four males at Tatarka Hill on the Upper Yenisei, approximately 2,000 km to the east, are likewise entirely Yakutia_LNBA and all carry Y-haplogroup N-L1026 (Zeng et al. 2025)—provides a plausible population-level context for the non-distance-decay pattern in our Mantel analyses. Zeng et al. (2025) show that Steppe_MLBA populations in Eastern Europe and Western Siberia as late as the middle Bronze Age carry no Yakutia_LNBA ancestry, implying jump-dispersal rather than gradual spatial diffusion. Allentoft et al. (2024) provide relevant background: populations east of the Urals maintained high internal relatedness until approximately 4,000 BP, consistent with localised groups whose technological traditions could remain stable between contacts. If templates were carried by these long-distance migrants, stone-tool morphologies could have leapt geographic distances without producing the isolation-by-distance gradient that our Mantel tests consistently fail to detect. The shared C1 type across the three genetically distinct Rostovka individuals (I32545/Yakutia_LNBA, I25555/C2a, I32898/R1a-Z645) supports this picture at the intra-site level: C1 has Eneolithic antecedents across the steppe corridor (Botai, Khvalynsk, Yamnaya), and its presence in burials of individuals from all three ancestry backgrounds is consistent with a template that was already pan-steppe before the ST network crystallised—carried by migrants from multiple directions rather than diffused gradually from a single point of origin. This mechanism is complementary rather than alternative to the aggregation-event model proposed in Section 4.3: both predict a non-clinal, locally structured morphological pattern. Zeng et al.'s (2025) conclusion that 'both cultural transmission and migration were key' is thus directly consistent with the dual-mechanism interpretation proposed on morphometric grounds.

Satyga XVI provides the only other site where our stone projectile dataset and the Zeng et al. (2025) aDNA dataset overlap directly. Both sequenced individuals (I32552, Burial 6; I32551, Burial 17) carry all three ancestry types—Yakutia_LNBA, Steppe_MLBA, and NEAHG—making Satyga-16 the most genetically admixed site in the entire

[1] Childebayeva et al. (2024) attribute the bone body armour to 'grave 34 (ROT016)' in their Discussion section. Examination of the primary excavation report (Matyushchenko and Sinitsyna 1988) indicates that the bone armour plates were recovered from Burial 33 (not Burial 34); the stone arrowheads from Burial 33 are illustrated on Fig. 67 of the same report and were assigned to Type C1 in the present study. Burial 33 corresponds to individual I32816 (ROT015; Y-haplogroup C2a) in the Zeng et al. (2025) AADR dataset (Supplementary Data 1). The grave numbering discrepancy between Childebayeva et al. (2024) and Matyushchenko and Sinitsyna (1988) may reflect a difference between the published excavation catalogue and the internal numbering system used in the aDNA study.

ST aDNA sample. Yet Satyga's stone projectile assemblage occupies an intermediate disparity position in our analysis, neither highly standardised nor highly heterogeneous. This discrepancy—maximum genetic admixture but only intermediate morphological diversity—may reflect the small aDNA sample (n = 2) or may indicate that genetic admixture and technological template diversity operate on different timescales or through different social mechanisms. Two constraints bound all inter-dataset comparisons presented here: the aDNA record comprises only 16 ST-period individuals across four sites, against 420 stone projectile specimens from ten sites; and morpho-technological types are assemblage-level constructs that cannot be attributed to individuals without direct grave-level analysis. Within these limits, the convergent evidence from morphometrics and ancient genomics is consistent with a Seima–Turbino world in which individuals of diverse ancestral backgrounds participated in shared technological traditions while maintaining locally distinct elaborations—a pattern most compatible with decentralised, apprenticeship-organised production that transcended, but was not indifferent to, the population boundaries visible in the genetic record.

4.5 Limitations

Several constraints bound the present conclusions. Reliance on published illustrations is the most fundamental: two-dimensional drawings ignore thickness and cross-sectional mass distribution, which may carry functional information, and Soviet-era reports vary in their drawing conventions and scale-bar precision. We assessed inter-report drawing consistency via residual analysis (see Materials) and found no significant report-level bias in outline structure, but this test cannot detect systematic biases introduced uniformly within a single report. Chronological control is coarse: available radiocarbon dates cannot resolve depositional sequences within individual cemeteries at the resolution needed to distinguish temporal from spatial patterning. The coding of discrete traits (tang shape, shoulder type) depends on the quality and completeness of site reports, which varies markedly across the dataset. Sample sizes range from 10 to 147 specimens; although we apply rarefied SoV disparity with bootstrap resampling, the Seima estimate (n = 10) carries wide confidence intervals and should be interpreted cautiously. Critically, the morpho-technological groups identified here are analytical constructs based on shape and attribute covariation. They should not be conflated with ethnic groups, archaeological cultures, or biological populations. The data establish that certain combinations of attributes co-occur with statistically significant site-level structure; they do not establish why producers chose those combinations, and they cannot distinguish learning-lineage effects from functional adaptation, personal choice, or raw-material constraints without independent evidence. In particular, the present dataset cannot disentangle functional optimisation—differences in penetration performance, target type, or haft-stress tolerance—from social transmission as drivers of the observed morphological variation; both mechanisms could independently produce the patterning documented here. Future work coupling morphometrics with raw-material sourcing, use-wear analysis, radiocarbon dating of individual burials, and bioarchaeological identity markers will be needed to move from descriptive typology to causal explanation.

5. Conclusion

This study presents the first quantitative morphometric classification of Seima–Turbino stone projectiles, based on 420 complete specimens from eight Seima–Turbino sites and two comparative assemblages. By combining outline-based geometry, mixed-data ordination, technological attribute coding and open R workflows, the analysis establishes a reproducible framework for comparing projectile forms across published site-report illustrations.

The analysis yields eleven reproducible morpho-technological types organised around two principal hafting templates: tanged and non-tanged. These types replace legacy site-specific labels with a cross-site classification based on shape and attribute covariation, while remaining practical enough to support field or museum attribution through a decision-tree key.

Site-level disparity and size variability distinguish relatively low- and high-variability assemblages. This pattern is consistent with differences in template control, depositional history, production scale and aggregation intensity, and it suggests that the Seima–Turbino lithic record was not produced by a single homogeneous craft regime.

Across four inter-site distance metrics, morphometric distances show no significant monotonic decay with geographic distance across the study region. The short-range negative autocorrelation observed in part of the distance analysis should remain provisional, but it indicates that geographically proximate sites could maintain distinct technological repertoires while sharing similarities with more distant assemblages.

The coexistence of multiple hafting templates within site assemblages, together with production-tool associations, is consistent with decentralised lithic production and distinct learning traditions. The contrast with more standardised bronze weapon production at some of the same sites highlights the value of treating stone projectiles as an independent line of archaeological evidence rather than as a subsidiary component of the bronze assemblage.

Cross-reference with published ancient DNA data provides a preliminary contextual check: the most widespread projectile type occurs among individuals representing three distinct ancestry components at Rostovka. This limited evidence does not demonstrate a general relationship between ancestry and technology, but it supports the interpretation that shared lithic practices could cut across biological descent categories.

The workflow developed here is directly applicable to museum collections and grey-literature assemblages for which direct remeasurement is difficult or impossible. Future work should integrate raw-material sourcing, use-wear analysis, direct radiocarbon dating of projectile-bearing burials and expanded bioarchaeological data to test whether the morphometric patterns identified here reflect production organisation, mobility, function or chronological mixing.

For Archaeological and Anthropological Sciences, the broader contribution is methodological as well as regional: image-based mixed-data morphometrics can turn legacy illustrations into reproducible datasets for evaluating technological variability, classification and transmission in archaeological contexts.

Statements and Declarations

Funding

The author did not receive support from any organisation for the submitted work.

Competing Interests

The author declares no competing interests.

Ethics approval and consent to participate

Not applicable. This study analyses published archaeological illustrations and derived morphometric data and did not involve new research with human participants, animals or sensitive cultural materials.

Author Contributions

Zhiping Yu (于之平): Conceptualisation, Data curation, Formal analysis, Investigation, Methodology, Software, Validation, Visualisation, Writing – original draft, Writing – review & editing.

Data Availability

The R analysis pipeline, including all processed specimen coordinate data, discrete morphological attribute codings, and site geographic coordinates, is archived on Zenodo and openly available at https://doi.org/10.5281/zenodo.20934739. The repository includes complete, runnable code for every analysis reported in this study. The latest version of the code is maintained at https://github.com/Zhiping-Yu-212/seima-turbino-pipeline. Original specimen line drawings, reproduced from published excavation reports under standard scholarly practice, are not redistributed in this repository; the archived dataset comprises the author's own derived measurements (elliptical Fourier coefficients, principal component scores, and discrete attribute codes) extracted from those published sources.

Supplementary Information

Online Resource 1 contains clustering sensitivity checks and full-sample classification diagnostics.

References

Agapov, S. A., Vasiliev, I. B., & Pestrikova, V. I. (1990). *Khvalynskiy eneoliticheskiy mogil'nik [Khvalynsky Eneolithic burial ground]*. Saratov University Press.

Allentoft, M. E., Sikora, M., Refoyo-Martínez, A., Irving-Pease, E. K., Fischer, A., Barrie, W., Ingason, A.,

Stenderup, J., Sjögren, K.-G., Pearson, A., Sousa da Mota, B., Schulz Paulsson, B., Halgren, A., Macleod, R., Schjellerup Jørkov, M. L., Demeter, F., Sørensen, L., Nielsen, P. O., Henriksen, R. A., ... Willerslev, E. (2024). Population genomics of post-glacial western Eurasia. *Nature, 625*(7994), 301–311. https://doi.org/10.1038/s41586-023-06865-0

Arkhipov, G. A., & Khalikov, A. Kh. (Eds.). (1978). *Arkheologiya i etnografiya Mariiskogo kraya, Vyp. 3: Lesnaya polosa Vostochnoi Evropy v Volosovsko-Turbinskoye vremya [Archaeology and ethnography of the Mari region, Issue 3: The forest belt of Eastern Europe in the Volosovo–Turbino period]*. Mari Research Institute.

Bader, O. N. (1962). *Turbinskii mogil'nik [Turbino cemetery]*. Nauka.

Bader, O. N. (1964). *Pervye metallurgi Urala [The earliest metallurgists of the Urals]*. Nauka.

Bader, O. N. (1970). *Bassein Oki v bronzovom veke [The Oka basin in the Bronze Age]*. Nauka.

Bader, O. N., Krainov, D. A., & Kosarev, M. F. (Eds.). (1987). *Epokha bronzy lesnoi polosy SSSR [The Bronze Age of the forest belt of the USSR] (Arkheologiya SSSR series)*. Nauka.

Besprozvanny, E. M., & Korochkova, O. N. (2011). *Satyga XVI: Seiminsko-trubinskii mogil'nik v taezhnoi zone Zapadnoi Sibiri [Satyga XVI: Seima–Turbino burial ground in the taiga zone of Western Siberia]*. Ekaterinburg–Surgut.

Bhattacharyya, A. (1943). On a measure of divergence between two statistical populations defined by their probability distributions. *Bulletin of the Calcutta Mathematical Society*, 35, 99–109.

Bleed, P. (1986). The optimal design of hunting weapons: Maintainability or reliability. *American Antiquity*, 51(4), 737–747. https://doi.org/10.2307/280862

Bonhomme, V., Picq, S., Gaucherel, C., & Claude, J. (2014). Momocs: Outline methods for the analysis of shapes in R. *Methods in Ecology and Evolution*, 5(11), 1106–1112. https://doi.org/10.1111/2041-210X.12278

Bourdieu, P. (1977). *Outline of a theory of practice*. Cambridge University Press.

Buchanan, B., & Collard, M. (2010). A geometric morphometrics-based assessment of blade shape differences among Paleoindian projectile point types. *Journal of Archaeological Science*, 37(2), 350–359. https://doi.org/10.1016/j.jas.2009.09.047

Cardillo, M., & Alberti, J. (2015). The evolution of projectile points and technical systems: A case from Northern Patagonian coast (Argentina). *Journal of Archaeological Science: Reports*, 2, 612–623. https://doi.org/10.1016/j.jasrep.2015.06.015

Chavent, M., Kuentz-Simonet, V., Labenne, A., & Saracco, J. (2014). Multivariate analysis of mixed data: The R package PCAmixdata. arXiv. https://arxiv.org/abs/1411.4911

Chernykh, E. N. (1992). *Ancient metallurgy in the USSR: The early metal age*. Cambridge University Press.

Chernykh, E. N., Hommel, P. N., & Savinetskaya, I. (Eds.). (2017). *Nomadic cultures in the mega-structure of the Eurasian world*. Academic Studies Press.

Chernykh, E. & Korochkova, O. & Orlovskaya, L.. (2017). Issues in the calendar chronology of the seima-turbino transcultural phenomenon. *Archaeology, Ethnology & Anthropology of Eurasia.* 45. 45-55. https://doi.org/10.17746/1563-0110.2017.45.2.045-055.

Childebayeva, A., Fricke, F., Rohrlach, A. B., Huang, L., Schiffels, S., Vesakoski, O., Mannermaa, K., Semerau, L., Aron, F., Solodovnikov, K., Rykun, M., Moiseyev, V., Khartanovich, V., Kovtun, I., Krause, J., Kuzminykh, S., & Haak, W. (2024). Bronze age Northern Eurasian genetics in the context of development of metallurgy and Siberian ancestry. *Communications Biology, 7*, 723. https://doi.org/10.1038/s42003-024-06343-x

Foote, M. (1997). The evolution of morphological diversity. *Annual Review of Ecology and Systematics*, 28, 129–152. https://doi.org/10.1146/annurev.ecolsys.28.1.129

Fox, A. N. (2015). A study of Late Woodland projectile point typology in New York using elliptical Fourier outline analysis. *Journal of Archaeological Science: Reports*, 4, 501–509. https://doi.org/10.1016/j.jasrep.2015.10.004

Gening, V. F., Zdanovich, G. E., & Gening, V. V. (1992). *Sintashta: Arkheologicheskie pamyatniki ariiskikh plemen Uralo-Kazakhstanskikh stepei [Sintashta: Archaeological sites of the Aryan tribes of the Ural-Kazakh steppes].* South Ural Book Publishing.

Golotvin, A. N., & Pryakhin, A. D. (2016). *Lipetskii kurgan – pamyatnik elity don-volzhskoi abashevskoi kul'tury [Lipetsk kurgan: An elite site of the Don–Volga Abashevo culture]*. Lipetsk.

Gower, J. C. (1971). A general coefficient of similarity and some of its properties. *Biometrics*, 27(4), 857–871.

Grushin, S. P., Kiryushin, Yu. F., Tishkin, A. A., Gorbunov, V. V., Kazakov, A. A., Dyadkov, P. G., Pozdnyakova, O. A., Solodovnikov, K. N., Tur, S. S., Potemkina, T. M., Bondarenko, A. V., Borisov, V. A., Kosintsev, P. A., Gayduchenko, L. L., Valkov, I. A., Milyaev, G. A., Sataeva, L. V., Volkov, P. V., Ponomareva, E. A., & Voronkin, K. I. (2016). *Eluninskiy arkheologicheskiy kompleks Teleutskiy Vzvoz-I v Verkhnem Priob'e: Opyt mezhdistsiplinarnogo izucheniya: Kollektivnaya monografiya [The Elunin archaeological complex Teleutsky Vzvoz-I in the Upper Ob region: An interdisciplinary study: Collective monograph]*. Izdatel'stvo Altaiskogo universiteta.

Guillerme, T., & Poisot, T. (2018). dispRity: A modular R package for measuring disparity. *Methods in Ecology and Evolution*, 9(7), 1755–1763. https://doi.org/10.1111/2041-210X.13022

Harush, O., Roux, V., Karasik, A., Grosman, L. (2020). Social signatures in standardized ceramic production – A 3-D approach to ethnographic data. *Journal of Anthropological Archaeology*, 60, Article 101213. https://doi.org/10.1016/j.jaa.2020.101213

Hegmon, M. (1992). Archaeological research on style. *Annual Review of Anthropology*, 21, 517–536.

Hess, T., Matzig, D., & Riede, F. (2025). Morphometric analyses of Late Palaeolithic and Early Mesolithic projectile points from Central Germany. *Lithic Technology*. Advance online publication. https://doi.org/10.1080/01977261.2025.2491158

Horn, J.L. A rationale and test for the number of factors in factor analysis. *Psychometrika* 30, 179–185 (1965). https://doi.org/10.1007/BF02289447

Kanivay, B. Y. (1964). *Kanninskaya peshchera [Kanning Cave]*. Nauka.

Kaufman, L., & Rousseeuw, P. J. (1990). *Finding groups in data: An introduction to cluster analysis*. Wiley.

Khalikov, A. K. (1966). *Pepkinskii kurgan [Pepkino kurgan]*. Mari Book Publishing.

Korochkova, O. N., Stefanov, V. I., & Spiridonov, I. A. (2020). *Svyatilishche pervykh metallurgov Srednego Urala [Sanctuary of the first metallurgists of the Middle Urals]* (E. N. Chernykh, Ed.). Izdatel'stvo Ural'skogo universiteta.

Krainov, D. A. (1963). *Pamiatniki fat'ianovskoi kul'tury: Moskovskaia gruppa [Monuments of the Fatyanovo culture: The Moscow group]*. Akademii Nauk SSSR.

Kuhl, F. P., & Giardina, C. R. (1982). Elliptic Fourier features of a closed contour. *Computer Graphics and Image Processing*, 18(3), 236–258.

Kuznetsov, P. F. (2004). *Pepkinskii kurgan as a reflection of confrontation at the dawn of a new Bronze Age epoch in Europe. In Voprosy arkheologii Urala i Povolzh'ya (No. 2, pp. 146–154).* Samara University.

Lagodovska, O. F., Shaposhnikova, O. G., & Makarevich, M. L. (1964). *Mykhailivs'ke poselennia [Mikhailivske settlement]*. Naukova Dumka.

Lave, J., & Wenger, E. (1991). *Situated learning: Legitimate peripheral participation*. Cambridge University Press.

Legendre, P., & Legendre, L. (2012). *Numerical ecology* (3rd ed.). Elsevier.

Lemonnier, P. (1992). *Elements for an anthropology of technology*. University of Michigan Press.

Lipo, C. P., Hunt, T. L., Horneman, R., & Bonhomme, V. (2016). Weapons of war? Rapa Nui mata'a morphometric analyses. *Antiquity*, 90(349), 172–187. doi:10.15184/aqy.2015.189

Liu, X. (2024). *Ouyà cǎoyuán shìyě xià de Sèiyīmǎ–Tú'ěrbīnnuò yǔ Zhōngguó [Seima–Turbino and China in the perspective of the Eurasian Steppe]*. Shanghai Guji Press.

Mantel, N. (1967). The detection of disease clustering and a generalized regression approach. *Cancer Research,* 27(2), 209–220.

Matyushchenko, V. I., & Sinitsyna, G. V. (1988). *Mogil'nik u sela Rostovka pod Omskom [The cemetery near the village of Rostovka near Omsk]*. Tomsk University Press.

Matzig, D. N. (2021). outlineR: An R package to derive outline shapes from (multiple) artefacts on JPEG images (Version 0.1.0) [Computer software]. Zenodo. https://doi.org/10.5281/zenodo.4527470

Merpert, P. Y. (1961). *Abashevskaya kul'tura Srednego Povolzh'ya [The Abashevo culture in the Middle Volga region]*. Nauka.

Molodin, V. I. (2012). Pamyatnik Sopka-2 na reke Omi, Tom 3 [Archaeological site of Sopka-2 on the Om River, Book 3]. IAET SB RAS.

Molodin, V. I., & Glushkov, I. G. (1989). *Samus'kaya kul'tura v Verkhnem Priob'e [The Samus culture in the Upper Ob' region]*. Nauka.

Molodin, V. I., & Grishin, A. E. (2016). *Pamyatnik Sopka-2 na reke Omi, Tom 4 [The Sopka-2 monument on the Om River, Vol. 4]*. IAET SB RAS.

Moreno, J. C., Bradley, B., Okumura, M., & Williams, T. J. (2022). Two Technological Traditions of Bifacial Points from the Breach Farm Site, Wales: An Interdisciplinary Analysis of Lithic Technology Integrating Experimental Replication, X-Ray Fluorescence, and Geometric Morphometry. Ethnoarchaeology, 14(1), 51–75. https://doi.org/10.1080/19442890.2022.2095843

Nelson, M. C. (1991). *The study of technological organisation. In M. B. Schiffer (Ed.), Archaeological method and theory* (Vol. 3, pp. 57–100). University of Arizona Press.

Nicolas, C. (2016). *Flèches de pouvoir à l'aube de la métallurgie de la Bretagne au Danemark (2500–1700 av. n. è.) [Arrows of power at the dawn of metallurgy from Brittany to Denmark]*. Sidestone Press.

Okladnikov, A. P. (1955). *Neolit i bronzovyi vek Pribaykal'ya, Chast' 3: Glazkovskii period [Neolithic and Bronze Age of the Baikal region, Part 3: Glazkovo period]*. Nauka.

Petřík, J., Sosna, D., Prokeš, L., Štefanisko, D., Galeta, P. (2018). Shape matters: Assessing regional variation of Bell Beaker projectile points in Central Europe using geometric morphometrics. *Archaeological and Anthropological Sciences*, 10(4), 893–904. https://doi.org/10.1007/s12520-016-0441-y

Robert, P., & Escoufier, Y. (1976). A unifying tool for linear multivariate statistical methods: The RV-coefficient. *Applied Statistics*, 25(3), 257–265.

Rousseeuw, P. J. (1987). Silhouettes: A graphical aid to the interpretation and validation of cluster analysis. *Journal of Computational and Applied Mathematics*, 20, 53–65.

Roux, V., & Courty, M.-A. (2019). *Ceramics and society: A technological approach to archaeological assemblages*. Springer.

Schiffer, M. B. (1996). *Formation processes of the archaeological record*. University of Utah Press.

Serikov, Yu. B. (2013). *Ozero Shaitanskoye — svyashchennoe ozero drevnosti [Shaitanskoye Lake: Sacred lake of antiquity]*. RSVPU Press.

Shennan, S. (2001). Demography and cultural innovation: A model and its implications for the emergence of modern human culture. *Cambridge Archaeological Journal*, 11(1), 5–16.

Sisk, M. L. (2013). European *Upper Paleolithic stone tool typology: An annotated translation of the de Sonneville-Bordes and Perrot typology* [Unpublished manuscript]. University of Notre Dame, CurateND Repository. https://doi.org/10.7274/R03R0QR2

Solovyev, B. S. (2005). The Yurinsky (Usty-Vetluzhsky) cemetery (results of excavations 2001–2004). *Rossiiskaya Arkheologiya*, 4, 103–112.

Stout, D. (2002). Skill and cognition in stone tool production: An ethnographic case study from Irian Jaya. *Current Anthropology*, 43(5), 693–722. https://doi.org/10.1086/342638

Vandkilde, H. (1996). *From stone to bronze: The metalwork of the Late Neolithic and earliest Bronze Age in Denmark* (P. Northover, Contributor). Jutland Archaeological Society.

Wiessner, P. (1983). Style and social information in Kalahari San projectile points. *American Antiquity*, 48(2), 253–276.

Wills, M. A., Briggs, D. E. G., & Fortey, R. A. (1994). *Disparity as an evolutionary index. Paleobiology*, 20(2), 93–130.

Wobst, H. M. (1977). *Stylistic behavior and information exchange*. In C. E. Cleland (Ed.), For the director: Research essays in honor of J. B. Griffin (pp. 317–342). University of Michigan Press.

Zaibert, V. F., & Khazbulatov, A. R. (Eds.). (2018). S*akral'nye konteksty Botaiskoi kul'tury [Sacred contexts of the Botai culture]*. Kazakh Research Institute of Culture.

Zeng, T. C., Vyazov, L. A., Kim, A., Flegontov, P., Sirak, K., Maier, R., Lazaridis, I., Akbari, A., Frachetti, M., Tishkin, A. A., Ryabogina, N. E., Agapov, S. A., Agapov, D. S., Alekseev, A. N., Boeskorov, G. G., Derevianko, A. P., Dyakonov, V. M., Enshin, D. N., Fribus, A. V., ... Reich, D. (2025). Ancient DNA reveals the prehistory of the Uralic and Yeniseian peoples. *Nature, 644*(8075), 122–132. https://doi.org/10.1038/s41586-025-09189-3

Supplementary Files

This is a list of supplementary files associated with this preprint. Click to download.

- SupplementaryMaterial.docx